1
Electronic Process in Organic Solids

Hongzhen Lin, Fenglian Bai

Organic solids, in a broad sense, include all solid-state materials consisting of organic molecules or polymers, namely, compounds with carbon atoms as their essential structural elements [1]. Under this generic term, the category of organic solids covers a wide variety of natural solids such as wood and cotton, and industrial products such as plastics and rubber, many of which are insulators. The scope of this book, however, will be confined to the class of organic solids that can serve as active components in electronic or photonic devices. The functionalities of these materials are mainly based on their capability to carry and transport charges and neutral excitations. For simplicity, hereafter the term "organic solid" will refer specifically to those organic materials showing (semi)conductor properties in the form of crystals, thin films, or glassy state.

Electronic process in organic solids determines the properties of the materials and their potential applications in optoelectronic devices. It is a very complicated process, and has a close relationship with molecular electronic structures, molecular interactions, charge–charge coupling, charge–photon coupling, and exciton–photon coupling, and so on. Consequently, chemists find it difficult to understand due to the complication of electronic process in organic solids. At this point, electronic process will be expounded from the chemist's perspective in order to appreciate the basic concepts and the nature of this complicated process.

1.1
Introduction

Solid-state devices – especially transistors – play a crucial role in modern electronic technology. Whilst the dominant building materials in solid-state electronics are inorganic semiconductors such as silicon or germanium, organic solids – in particular, organic semiconductors – have emerged recently as a new class of electronic materials and have subsequently become a strong competitor of inorganic semiconductors in many aspects of the electronics industries [1]. The key advantages of organic solids over metals and inorganic semiconductors stem from their potential to combine the electrical properties of (semi)conductors with the

Organic Optoelectronics, First Edition. Edited by Wenping Hu.

properties typical of organics – that is, low cost, high processability, mechanical flexibility, and a versatility of chemical synthesis [2]. These materials provide the possibility to realize novel applications such as large areas, flexible displays, low-cost printed integrated circuits, and plastic solar cells [1]. During the past few decades, tremendous progress has been achieved along these lines, such that today a totally new field of research – organic electronics – has emerged and is continuing to develop.

The first realization that organic compounds could carry an electric current was made many years ago. Indeed, the first studies of the conductivity of anthracene crystals, as a prototype of organic semiconductors, date back to the early twentieth century [3, 4]. During the 1950s, various research teams found that polycyclic aromatic compounds could form semi-conducting charge-transfer complex salts with halogens; notably, a high conductivity of $0.12\,S\,cm^{-1}$ was reported in a perylene–iodine complex in 1954 [5]. Subsequently, during the 1960s molecular crystals aroused intense research interest, due to the discovery of electroluminescence [6, 7]. During the 1970s, the successful synthesis of conjugated polymers, and the observation of a controllable conductivity over the range from insulating to metallic [8], led to the establishment of a second important class of organic semiconductors, for which the Nobel Prize in Chemistry was eventually awarded in 2000.

Along with great progress in the academic research of organic solids, tremendous technological developments have also been achieved in the creation of (opto) electronic devices from these materials. Ultimately, the door to "real" applications of organic semiconductors was opened in 1987 by Tang and VanSlyke who, while working at Kodak, successfully fabricated thin-film organic light-emitting diode (OLED) devices from tris(8-hydroxyquinolinato) aluminum (Alq_3), a π-conjugated molecular material [9]. Shortly thereafter, Friend and his group at the Cavendish Laboratory in Cambridge reported a highly efficient polymer-based OLED using a conjugated polymer, poly(*p*-phenylene vinylene) (PPV) [10]. Besides OLEDs, organic semiconductors are also used widely in other devices such as organic solar cells [11, 12], organic field-effect transistors (FETs) [13, 14], chemical sensors [15, 16], and organic lasers [17, 18]. Nowadays, the field of organic electronics has reached a new era and is facing a bright future of industrialization. In particular, OLEDs have made a solid step towards the commercial market, having shown great potential for use in panel displays, digital cameras and mobile phones, and for white light illumination.

Nonetheless, much hard work lies ahead before the large-scale production of organic electronic devices becomes possible, and this will require the extensive collaboration of physicists, chemists, and engineers. Although an incessant effort will clearly be required to develop device fabrication techniques, the most fundamental approach for improving device performance is to create new organic solids with optimal properties as desired. Yet, this raises a major challenge for both organic and materials chemists alike since, in order to guide the design and synthesis of novel materials, it is crucial to acquire a better fundamental understanding of the nature of electronic excitations, charge carriers, and transport

phenomena in organic solids [2]. To date, many experimental and theoretical studies have been conducted for this purpose, and comprehensive reviews of the topic are available in books and journals [1, 2, 19–22]. Unfortunately, however, the theoretical interpretations and physical models of organic solids are often "too abstract" for synthetic chemists to understand. Consequently, in this chapter the basic concepts will be introduced from a chemist's perspective, allowing them to capture the nature of the complicated electronic processes in these materials. The chapter is organized as follows: the molecular and supramolecular structural features of some prototype organic solids are described in Section 1.2, after which the fundamental photophysical properties of organic conjugated molecules are introduced in Section 1.3. In Section 1.4, details of the neutral and charged excited states in conjugated polymers are provided, while in Section 1.5 a brief discussion is provided of charge carrier generation and transport in organic solids.

1.2
Structure Characteristics and Properties of Organic Solids

An atom consists of a positively charged nucleus and one or more electrons that are bound by the electric field of the nucleus. In a system having more than one atom, an electron is not necessarily bound to one nucleus but can be shared between different atoms, depending on the interatom interactions and the energy state of the electron. In metals and inorganic semiconductors, the strong interatomic electronic interactions facilitate the delocalization of outer shell electrons over a large number of atoms. But, the situation in organic solids is very different where, depending on the nature of intermolecular interactions, organic solids can be classified into two types [2].:

- In *nonpolar organic solids*, the molecules are held together by van der Waals interactions, which are rather weak compared to covalent bonding. The physical properties of nonpolar organic solids are only slightly changed relative to those of the free molecules, since the intramolecular interactions are dominant.
- *Polar organic solids* are organic solid materials where both ionic bonding and van der Waals forces exist. Examples of this type include organic charge-transfer complexes and radical-ion salts, in which the positive and negative charges are separated and located on different molecules. Nevertheless, the ionic bonding in these ionic molecular crystals is weaker than that in inorganic salts, as molecules are larger than atoms.

Among organic solids can be included photoconductive materials, conductive polymers, electroluminescent materials, and photovoltaic materials, the functionality of which depends essentially on their molecular structures. Although a wide variety of organic semiconductors and conductors have been described, they include in common a conjugated π-electron system in the skeletal structure of the

constituent molecules. Typically, a conjugation system is composed of alternating single and multi bonds in which π-electrons are delocalized over the connected p_z-orbitals of contiguous sp^2-hybridized carbon atoms. Other atoms with available p_z-orbitals may also be involved. The characteristic optical and electronic processes that occur in organic (semi)conductors are closely related to which type of conjugation systems are contained, and how those conjugation systems interact one with another. Hence, the feasibility of modifying and altering the conjugation system in a molecule by chemical synthesis offers a wide range of possibilities to tune the optoelectronic properties of these organic solids. Some important classes of organic solid are detailed in following subsections, according to the major conjugation systems that they contain.

1.2.1 Organic Solids

Organic solids are usually classified into two groups according to molecular weight: (i) conjugated small molecules; and (ii) conjugated polymers. Often, the conjugated moiety of a molecule is referred to as a chromophore, one or a few of which are typically contained in a small molecule. In conjugated polymers, the π-electron delocalization is often interrupted by intrinsic or dynamic defects in the polymer chains, and generally persists for only a few tens of repeating units [23]. Consequently, a long conjugated polymer chain can be regarded approximately as an ensemble of weakly coupled chromophores of relatively short conjugation lengths.

The key difference between conjugated polymers and small molecules lies in their crystallinity, and the way in which they are processed to form thin films. For example, small molecules tend to crystallize into ordered arrays when they are deposited from the gas phase by sublimation or evaporation, whereas conjugated polymers can only be processed from solution, such as by spin-coating or printing techniques, so that in general amorphous thin films are formed. The performance of an organic solid in a devices is found to be highly sensitive to the way in which the molecules are arranged in the thin films.

The molecular structures of several prototype organic solids are shown in Figure 1.1. The simplest conjugation system is present in polyenes – compounds which contain one or more sequences of alternating double and single carbon–carbon bonds. A well-known example of this is *trans*-polyacetylene (t-PA) which, despite having the intrinsic properties of an insulator, has demonstrated an enhanced conductivity via chemical reduction/oxidation (redox) [8]. In fact, this finding proved to be a milestone in the development of organic electronic materials, such that the Nobel Prize for Chemistry was awarded to Alan Heeger, Alan MacDiarmid, and Hideki Shirakawa in 2000 for their pioneering research on t-PA and other conductive polymers.

Poly-aromatic hydrocarbons (PAHs) and their substituted derivatives represent another typical class of organic solid, with well-studied examples including anthracene, rubrene, pentacene, fluorene, pyrene, perylene, and coronene. These com-

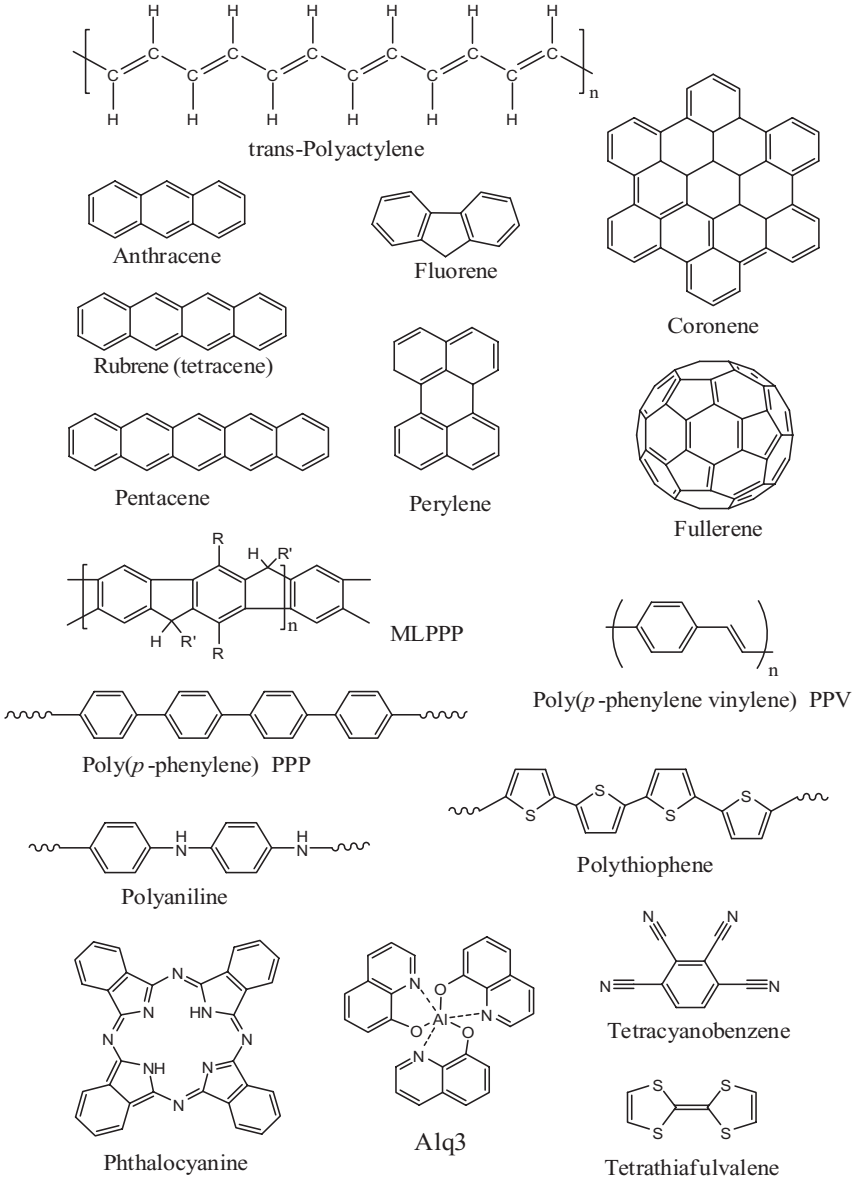

Figure 1.1 Molecular structures of some prototypes of organic solids.

pounds consist of fused aromatic rings, and are recognized as harmful pollutants to the air. Yet, in contrast they have been shown to be good candidates for the construction of electronic devices, with high charge mobilities having been reported in crystallized films of rubrene, pentacene and their derivatives, confirming their potential as organic FETs [24].

Currently, PAHs are also used extensively in OLEDs [25] as emissive dopants or charge-transporting materials. For example, polyacenes such as naphthalene, anthracene, rubrene, and pentacene are frequently employed as model systems in molecular physics and solid-state physics investigations, due to their simple linear structure, their defined conjugation lengths, an ability to form highly ordered crystals, and their well-determined optical and electronic properties. A linear extension of such a fused-ring structure can be demonstrated in ladder-type conjugated polymers, such as methyl-substituted ladder-type poly-*para*-phenylene (MLPPP) [26]. It is also worth noting here that all-carbon materials such as fullerene, carbon nanotubes and graphene, can be visualized as extended PAHs.

Many organic solids are produced from other aromatic hydrocarbons, and in such compounds the conjugation system typically consists of multiple aromatic rings that are connected with each other via a single bond, or through a vinylene or ethynylene group. Conjugated polymers such as poly (*p*-phenylene) (PPP), PPV, and poly (*p*-phenylene ethynylene) (PPE) belong to this group.

Conjugation systems containing heteroatoms such as sulfur and nitrogen are very useful building blocks for organic semiconductors, as the heteroatoms can be incorporated either outside or inside of the aromatic rings. Polyaniline and poly(*p*-phenylene sulfide) are examples of the "outside" case, while the "inside" case includes polythiophene and polypyrrole. As a special type of heteroaromatic compound, tetrapyrrole macrocycles including phthalocyanines, porphyrins and porphyrazines have also been investigated in organic electronics and photonics [27, 28], often appearing as complexes with metals such as copper and zinc.

Other types of organic metal complex have also been identified, a good example being the above-mentioned compound, Alq_3; organic complexes of other metals such as Zn, Pt, Os, Eu, and Ir were also reported [29, 30]. Alq_3 and its derivatives are important electroluminescent materials for OLEDs, and are also used as electron-transporting materials in photovoltaic devices such as solar cells.

In some cases, two different aromatic compounds can form charge-transfer complex crystals with a fixed uniform composition, much like a new compound. When the charge transfer occurs only in an electronically excited state, these are termed "weak" donor–acceptor (D–A) crystals; a good example is anthracene–tetracyanobenzene (TCNB). In the strong D–A complexes, the charge transfer takes place in the electronic ground state; a well-studied example is the compound tetrathiafulvalene–tetracyanoquinodimethane (TTF:TCNQ) [1].

Although, so far, attention has been focused on the skeletal structure of molecules, the conjugated backbones are often decorated with a variety of side groups. These side substituents not only improve the solubility of a compound but also greatly impact on the optical and electronic properties of the material. For instance, the π-π^* energy gap of an aromatic compound can be tuned by introducing electron-donating or withdrawing substituents. Bulky side groups can reduce the formation of non-emitting interchain aggregates in conjugated polymers [31].

Inorganic semiconductors may be either *p*-type or *n*-type, depending on which type of dopant is used. The dominant charge carriers are holes in the *p*-type semiconductors, but electrons in the *n*-type. Likewise, organic semiconductors may also

be classified as *p*-type and *n*-type, corresponding to hole-transporting and electron-transporting materials, respectively. It should be noted that the mechanism lying behind this classification of organic semiconductors is actually different from that used for their inorganic counterparts. Whether an inorganic semiconductor is *n*- or *p*-type is determined by the extrinsic dopants, whereas in the case of organic semiconductors this depends much more on the intrinsic chemical structures of the materials. For example, aryl amines are typical hole-transporting materials, whilst Alq_3 is a characteristic electron-transporting material. It should be noted that some organic semiconductors, such as PPVs, possess both hole- and electron-transporting abilities, and consequently their roles in devices will vary from case to case.

1.2.2
Molecular Geometries

The molecules or polymer chains that constitute organic solids may have various geometries. For example, a linear backbone can be found in polyacetylene and PPV, while phthalocyanines adopt a two-dimensional (2-D) planar structure. Organic solids have also been reported with other molecular geometries (Figure 1.2), including star-shaped structures [32], tree-shaped structures such as dendrimers [33] and hyperbranched polymers [34], as well as spiro compounds [35] in which two rings are connected through just one atom. The geometry has a significant effect on the conjugation length, the rigidity, the conformational variety, and the assembling behavior of a molecule, and thus greatly influences the properties of the compound in the solid state.

1.2.3
Aggregations and Assemblies

It should be borne in mind that organic conjugated compounds are used in opto-electronic devices as condensed solid films, but not as independent free molecules.

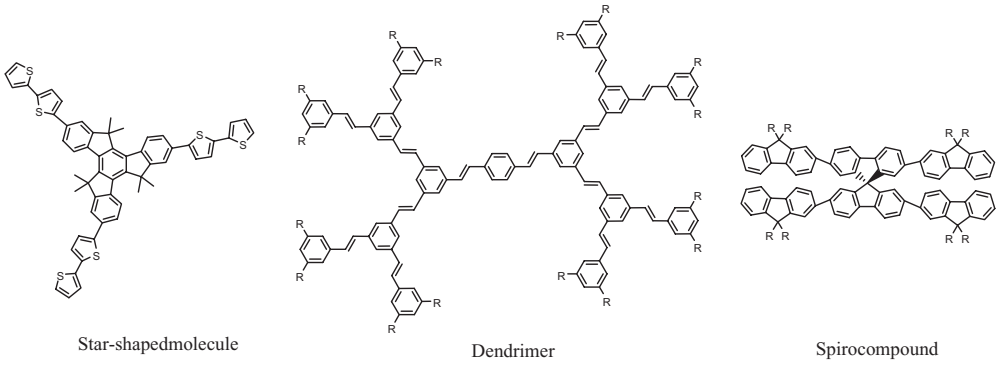

Figure 1.2 Several different geometries of conjugated molecules.

The intermolecular forces are crucial for the optical and electronic processes that occur therein, with the effect being either positive or negative depending on the usage. For instance, an efficient π-π stacking is usually good for charge transport, and thus an advantage if the material is to be used in FETs. On the other hand, π-π stacking often results in a quenching of emissive excited states, and therefore should be avoided when the compound is to be used as an electroluminescent material in OLEDs. Intermolecular forces other than π-π stacking include hydrogen bonding, electrostatic forces, and hydrophobic/hydrophilic effect, and these play important roles when the molecules are aggregated or assembled to form a solid thin film. In return, the ultimate morphology of the thin film has a great effect on the way that the molecules interact. In fact, the cooperation mechanism of various intermolecular interactions during molecular assembly, and its effect on device performance, is currently a "hot topic" of research in this field.

1.3 Electronic Processes in Organic Small Molecules

The complex intra- and intermolecular interactions in organic solids create major problems in the mathematical modeling of these materials. Indeed, in order to understand the large-scale properties of organic solids, it is necessary first to have an insight into their molecule-scale properties. Initially, it is both convenient and practical to consider simple model systems, before turning to more complicated cases. In this section, some fundamental optical and electronic processes that take place in an individual molecule, or between two molecules, and which have been investigated for many centuries, will first be revised. In particular, interest will be focused on processes as photogeneration and the relaxation of electronic excited states, and photoinduced charge/energy transfer.

1.3.1 Photophysics of Small Molecules

1.3.1.1 Molecular Orbital Model

A spatially confined particle can only take on certain discrete values of energy, and an electron bound to atoms or molecules falls into this case. These discrete values are termed "energy levels," and in quantum mechanics the states of electrons in atoms or molecules are described by so-called "wavefunctions." Here, the molecular orbital (MO, a model that is much more familiar to chemists) will be used, as MOs represent mathematically the regions in a molecule where an electron is most likely to be found. Any electronic state of a molecule can be described by a certain linear combination of its MOs. According to the Pauli principle, one MO can accommodate at most two electrons; hence, if a MO is fully occupied the two electrons therein must have opposite spin directions. The ground state of the molecule can be reconstructed by filling its electrons to the first few lowest energy MOs, while following the Pauli principle. The π-orbitals of benzene are shown as

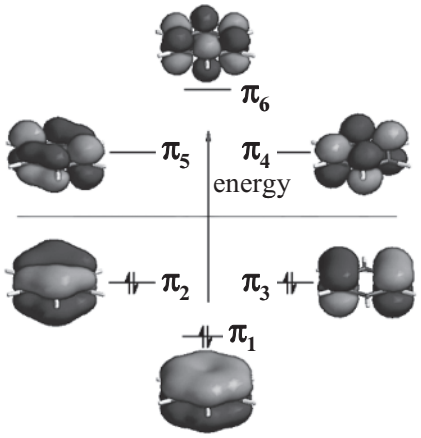

Figure 1.3 π-orbits of benzene. At ground state, the electrons first fill the lower-energy orbits.

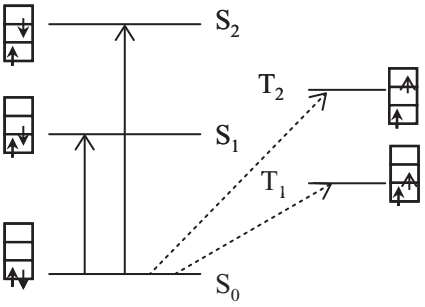

Figure 1.4 A simplified Jablonski diagram of an organic molecule. Solid arrows indicate spin-allowed transitions; dotted arrows indicate spin-forbidden transitions. S, singlet; T, triplet.

an example in Figure 1.3. The electronic transition of a molecule can be expressed as the moving of an electron from one MO to another.

1.3.1.2 **Jablonski Diagram**

Light absorption and emission processes are usually illustrated by the Jablonski diagram, in which the electronic states are vertically arranged according to the relative energy level. A simplified Jablonski diagram for a molecule that is free from intermolecular interactions is shown in Figure 1.4. Such an ideal case can be approximated in gas or in diluted solutions of the molecules in inert solvents.

Not all of the molecular orbitals take part in the light absorption and emission transitions; rather, these transitions are usually dominated by the highest occupied

molecular orbital (HOMO) and the lowest unoccupied orbital (LUMO). It should be noted that HOMO and LUMO are defined corresponding to the ground state of a molecule. Commonly, the ground state of an organic molecule is a singlet state in which the HOMO is fully occupied by two electrons of opposite spin. One of the two electrons is then promoted to LUMO or a higher energy level, when the molecule absorbs a photon of proper energy. In most cases, the excited electron will maintain its original spin, resulting in a singlet excited state. In Figure 1.4, the singlet ground, first, and second electronic states are depicted by S_0, S_1, and S_2, respectively. In some rare cases, the excited electron may change its spin direction and a triplet excited state will be then formed (denoted as T_1 and T_2, etc.). Triplet states generally cannot be directly accessed from S_0. An excited state can return to the ground state by emitting a photon of certain energy.

For organic molecules containing a π-conjugated system, the π-bonding is significantly weaker in comparison to the σ-bonds that form the backbone of the molecules. Therefore, the lowest electronic excitations of conjugated molecules are the π-π* transitions, with an energy gap typically between 1.5 and 3 eV, leading to light absorption or emission in the visible spectral range. The energy gap of an organic molecule can be controlled by changing the size of the conjugation system. Typically, the energy gap decreases with increasing conjugation length.

1.3.1.3 Frank–Condon Principle

The energy level scheme in Figure 1.4 does not take into account the motion of the nuclei relative to the molecular coordinate. The displacement of nuclei also corresponds to a series of discrete energy levels, but with a much smaller spacing than the electronic levels; these are termed vibrational energy levels. Each electronic state possesses a series of possible vibrational states; hence, vibrational transition can be thermally activated, and hence a molecule will have the probability to remain at a higher vibrational level, depending on the temperature. To account for this effect, the first few vibration energy levels associated with each electronic state are included into the Jablonski diagram (Figure 1.5, depicted by 0,

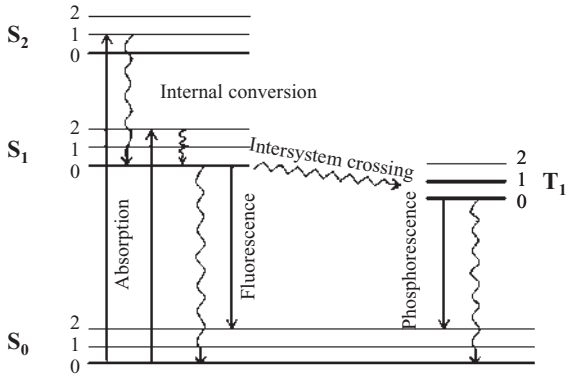

Figure 1.5 Energy level schemes and transitions of an organic molecule. S, singlet; T, triplet.

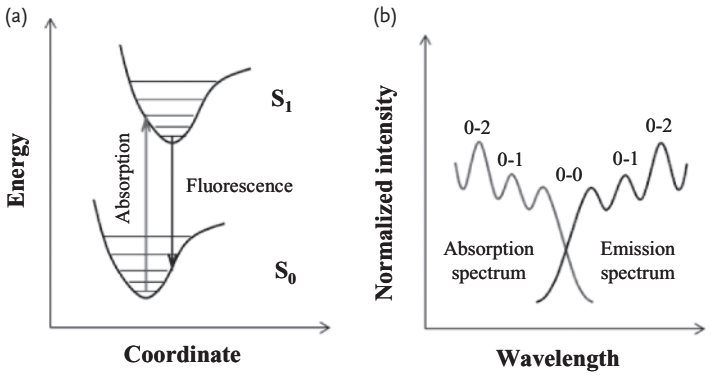

Figure 1.6 (a) Schematic illustration of the Frank–Condon principle. The most probable electronic transition occurs without a change of nuclei coordinates; (b) Schematic illustration of the mirror-image rule.

1, 2, etc.) [36]. At room temperature, the thermal energy is inadequate to significantly populate the excited vibrational states. Absorption and emission occur mostly from molecules with the lowest vibrational energy. The transition between the lowest vibrational levels of the electronic states, for example, between $S_0(0)$ and $S_1(0)$, is termed 0-0 transition.

At this point, it may help to introduce the Frank–Condon principle, which states that an electronic transition is most likely to occur without changes in the positions of the nuclei in the molecule and the surrounding environment. The quantum mechanics description of the principle is that, during an electronic transition, a change from one vibrational energy level to another will be more likely to occur if the two vibrational wavefunctions overlap more significantly. Hence, if the potential energy curves (system energy versus nuclei coordinate) of the initial and final electronic states are plotted, a Frank–Condon transition can be depicted as a vertical line between the two curves, in correspondence to an unchanged coordinate during the transition (Figure 1.6). For this reason, Frank–Condon transition is often termed vertical transition. In the Jablonski diagram, electronic transitions between states are also drawn as vertical lines to illustrate the vertical nature of the transitions. According to the Frank–Condon principle, 0-0 transition is generally not the most probable transition, as the thermally equilibrated molecular geometry (coordinate) of an electronic excited state is often different from that of the ground state.

1.3.1.4 Electronic Absorption

The transition from S_0 to S_1 or higher singlet states is spin-allowed. Such a photon absorption process takes place very rapidly, typically at a time scale of femtoseconds (10^{-15} s). The electronic absorption of a substance at certain light wavelength follows the Lambert–Beer law:

$$I = I_0 e^{-\varepsilon Cl} \tag{1.1}$$

where I_0 and I are the intensity of the incident light and the transmitted light, respectively, ε is the molar extinction coefficient, C is the molar concentration of the molecule, and l is the distance that the light travels through the material.

Equation (1.1) is frequently used for solutions, where l is the thickness of the solution in the light path. For molecular crystals and for thin films consisting of one compound, the concentration C is a constant that depends on the density of the material and the molecular mass. In such cases, the product of ε and C can be replaced by one constant k – that is, $I = I_0 e^{-kl}$ – where l is the thickness of the crystal or film. More generally, the Lambert–Beer law can be expressed as

$$I = I_0 e^{-\sigma N l} \tag{1.2}$$

where σ is the absorption cross-section of a single molecule and N is the density (number per unit volume) of absorbing molecules. Defining $A = \log(I_0/\mathrm{I})$ leads to

$$A = \log(I_0/I) = \ln 10 \varepsilon C l = \varepsilon' C l \tag{1.3}$$

where A is termed absorbance, a parameter that is proportional to the concentration of the absorbing molecules. Equation (1.3) is often used to measure the concentration of a substance in solution or in a solid matrix.

The molar extinction coefficient ε (or the molecular absorption cross-section σ) varies with the light wavelength or frequency. The theoretical interpretation of absorption is nontrivial, but some simple facts should be mentioned at this point. First, in order to excite a molecule, the energy of the incident photon (given by $E = \mathrm{h}\upsilon$, where $\hbar$ is Plank's constant and υ is the light frequency) must match the energy gap between the initial state and the final state. This means that only light with certain frequencies (or wavelengths) can be absorbed by the molecule. Second, electronic transition (like absorption) can be seen as a displacement of the negative charge center relative to the positive charge center of the molecule. Hence, a chromophore can be approximately treated as a dipole oscillator with a certain resonance frequency.

The absorption spectrum can be monitored by recording the absorbance as a function of the wavelength (or frequency) of the incident light. The electronic absorption of atoms and molecules generally lies in the ultraviolet or visible region; hence, it is often referred to as "UV-visible absorption." Because of the involvement of vibrational energy levels, different absorption bands may be observed in correspondence to the energy gap between 0-0, 0-1, and 0-2, etc.; this is known as the vibrational structure of the absorption spectrum. The absorption spectrum of an organic compound in a gas state often appears as a series of sharp lines that are greatly broadened in solution because of perturbations from the surrounding solvent molecules; even broader absorption bands may be identified for an amorphous solid. In contrast, molecular crystals often show narrow absorption lines similar to those of a gas, but with a distinctive vibrational structure.

Following light absorption, a molecule is usually excited to a higher vibrational level of either S_1 or S_2. Except for a few rare cases, excited molecules rapidly relax to the lowest vibrational level of S_1; this process is termed internal conversion, and generally occurs within 10^{-12} s or less.

1.3.1.5 Fluorescence and Phosphorescence

Electronic transition from S_1 to S_0 is also spin-allowed; this transition can occur spontaneously by the emission of one photon, when the emitted light is termed fluorescence [36]. A molecule may stay at S_1 for a brief moment before it returns to the ground state; the average time that a molecule spends between its excitation and its return to the ground state is referred to as the fluorescence lifetime, and for a conjugated compound this lies in the range of 10^{-9} to 10^{-8} s. Fluorescence emission generally results from the lowest energy vibrational state of S_1, as the internal conversion (10^{-12} s) is generally complete prior to emission. Following fluorescence emission, the molecule typically returns to a higher vibrational energy level of S_1, which then quickly relaxes to the lowest energy vibrational state through an internal conversion. The return to an excited vibrational state at the level of the S_0 state results in a vibrational structure in the emission spectrum. The fluorescence emission spectrum is a plot of fluorescence intensity as a function of emission wavelength or frequency, in which case the wavelength of the excitation light is fixed. It is also possible to record the fluorescence intensity at a certain emission wavelength while scanning the excitation wavelength, when the resultant spectrum – the fluorescence excitation spectrum – is an analog of the absorption spectrum.

Fluorescence typically occurs at lower energies or longer wavelengths than absorption. This is easy to understand, as some of the excitation energy will be lost during the rapid thermal relaxation of S_1 from higher energy vibrational levels to the lowest, and further lost when S_1 decays to higher vibration levels of S_0. The difference (in wavelength or frequency units) between the positions of the band maxima of the absorption and emission spectra is termed the Stokes shift [36].

With some exceptions, the fluorescence emission spectrum is typically a mirror image of the absorption spectrum of the $S_0 \rightarrow S_1$ transition (see Figure 1.6b). This similarity occurs because electronic excitation does not greatly alter the nuclear geometry; hence, the spacing of the vibrational energy levels of the excited states is similar to that of the ground state. According to the Franck–Condon principle, all electronic transitions occur without any change in the position of the nuclei. Therefore, if a particular transition probability between the 0th and 1st vibrational levels is the largest in absorption, the reciprocal transition is also the most probable in emission. As a result, the vibrational structures seen in the absorption and the emission spectra are similar. For the absorption band of $S_0 \rightarrow S_2$ transition, the corresponding mirror-image emissive band does not exist due to a rapid internal conversion from S_2 to S_1.

An important parameter used to characterize fluorescence is the fluorescence quantum yield (Φ), which is the ratio of the number of photons emitted to the number absorbed. The S_1 state may have decay pathways other than fluorescence, and this leads to Φ values lower than 1. Typically, Φ can be expressed as follows:

$$\Phi = k_f / (k_f + k_{nr}) = \tau / \tau_n \tag{1.4}$$

where k_f is the fluorescence emission rate constant of the S_1 state, and k_{nr} is the non-irradiative decay rate constant of S_1, while $\tau = 1/(k_f + k_{nr})$ is the fluorescence

lifetime of the molecule, and $\tau_n = 1/k_f$ is termed the natural lifetime; that is, the fluorescence lifetime in the absence of non-irradiative decay.

If any additional nonirradiative decay pathway is introduced to the molecules, it will result in a decrease of the fluorescence quantum yield; this is termed fluorescence quenching. If the additional nonirradiative decay is caused by a quencher with a quenching rate constant of k_Q, then it is possible to write:

$$\Phi = k_f/(k_f + k_{nr} + k_Q[Q]) = \Phi_0(k_f + k_{nr})/(k_f + k_{nr} + k_Q[Q]) = \Phi_0/(1 + K[Q]) \tag{1.5}$$

where Φ and Φ_0 are the fluorescence quantum yield of the quenched and unquenched sample, respectively, $K = k_Q/(k_f + k_{nr})$ is called the Stern–Volmer quenching constant, and $[Q]$ is the concentration of the quencher. Equation (1.5) is usually expressed in the following form:

$$F_0/F = \Phi_0/\Phi = 1 + K[Q] \tag{1.6}$$

This is the famous Stern–Volmer equation [36], in which F_0 and F are the fluorescence intensity of the unquenched and quenched sample, respectively. This equation is valid for dynamic quenching caused by diffusion-controlled collisions between the fluorophores and quenchers. For static quenching, where a fraction of the molecules are completely quenched as a result of forming nonirradiative stable complexes with quenchers while the others are unaffected, then Eq. (1.6) is still operational but the physical meaning of K is different. For dynamic quenching, the fluorescence lifetime is shortened, whereas for static quenching an unchanged fluorescence lifetime will be observed in correspondence to the fraction of unaffected molecules.

Molecules in the S_1 state can also undergo a spin conversion to the first triplet state T_1. Emission from T_1 is termed phosphorescence, and is generally shifted to longer wavelengths (lower energy) relative to the fluorescence. The conversion of S_1 to T_1 is referred to as intersystem crossing. The transition from T_1 to S_0 is spin-forbidden, and as a result the rate constants for triplet emission are several orders of magnitude smaller than those for fluorescence. The T_1 state typically has a relatively long lifetime, ranging from 10^{-3} to 1 s. Phosphorescence is often too weak to be observed at room temperature; however, the phosphorescence quantum yields can be enhanced by incorporating heavy atoms such as bromine and iodine into the molecules. These heavy atoms facilitate intersystem crossing due to spin–orbit coupling, with high phosphorescence quantum yields being achieved in some metal complexes.

In some cases, an excited molecule and an adjacent ground-state molecule can form an instantaneous complex that emits fluorescence at a longer wavelength (i.e., lower energy) than the excited molecule itself. This complex is called an excimer [37] if the two molecules are of the same type, but an exciplex [38] if the two molecules are different. For example, pyrene forms an excimer in concentrated solution, while anthracene can form an exciplex with aniline. The emission bands of the excimer and exciplex are typically broad and structureless. The

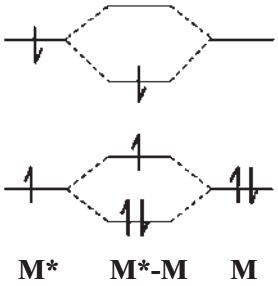

Figure 1.7 Molecular orbital splitting during excimer formation. The excimer emits at a longer wavelength because of a decreased energy gap.

excimer and exciplex are weak charge-transfer complexes having lifetimes of about 10^{-9} s; typically, these complexes dissociate when they return to the ground state. The involved photophysical processes can be expressed as follows.

$D + \hbar\upsilon \rightarrow D^*$ – molecule D absorbs one photon and jumps to excited state

$D^* \rightarrow D + \hbar\upsilon_F$ – the excited state emits one photon (fluorescence) and returns back to ground state

$D^* + A \rightarrow (DA)^*$ – the excited state D* forms a complex with a ground-state molecule A

$(DA)^* \rightarrow D + A + \hbar\upsilon_{FE}$ – the complex emits one photon ($\nu_{FE} < \nu_F$) and returns back to ground state

where D and A can be either the same or different molecules.

The formation of an excimer or exciplex is the result of a charge redistribution between the excited molecule and the ground-state molecule. For such a process to occur, the two molecules must have some overlap between their π-orbitals. The longer wavelength emission of excimer/exciplex can explained as being a result of molecular orbital splitting (Figure 1.7).

1.3.2 Excitation for Charge and Energy Transfer in Small Molecules

1.3.2.1 Photoinduced Electron Transfer

Following excitation, one of the two electrons in the HOMO level jumps to LUMO, or an even higher energy level, so as to provide the molecule with a higher activity in the redox reaction. On the one hand, the excited electron gains more energy and hence becomes easier to be donated; on the other hand, the HOMO becomes only half-occupied and can accept one electron from a reductant. Such a light-driven reduction/oxidation process is termed photoinduced charge transfer (Figure 1.8). The formation of excimer or exciplex is a case of partial charge transfer, where the charge density is slightly redistributed between the two constituent molecules. In general, photoinduced charge transfer refers to the complete transfer of one

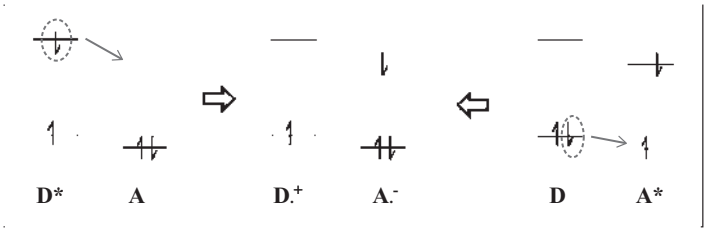

Figure 1.8 Schematic representation of photoinduced charge transfer between the donor (D) and acceptor (A).

charge entity (e.g., an electron or a proton) between two distinct atoms, functional groups, or molecules following photon absorption. At this point, attention will be focused on photoinduced electron transfer (PIET) between two molecules (intermolecular), or between two moieties of the same molecule. In such a process, the molecule or moiety providing an electron is called the donor (D), while the other molecule/moiety receiving the electron is called the acceptor (A). Typically, electron transfer results in the formation of a radical cation of the donor ($D^{\ddagger\bullet}$) and a radical anion of the acceptor ($A^{\bar{\bullet}}$). In general, PIET is a multi-step process, one possible mechanism of which is as follows:

$D + h\nu \rightarrow D^{S_1}$ – Excitation of D to singlet excited state
$D^{S_1} + A \rightarrow [D^{\delta+} \ldots A^{\delta-}]^S$ – Initial charge redistribution between D^{S_1} and A
$[D^{\delta+} \ldots A^{\delta-}]^S \rightarrow [D^{\ddagger\bullet} \ldots A^{\bar{\bullet}}]^S \rightarrow D^{\ddagger\bullet} + A^{\bar{\bullet}}$ – Charge transfer and separation
$D^{S_1} \rightarrow D^{T_1}$ – Conversion to triplet excited state via intersystem crossing
$D^{T_1} + A \rightarrow [D^{\delta+} \ldots A^{\delta-}]^T$ – Initial charge redistribution between D^{T_1} and A
$[D^{\delta+} \ldots A^{\delta-}]^T \rightarrow [D^{\ddagger\bullet} \ldots A^{\bar{\bullet}}]^T \rightarrow D^{\ddagger\bullet} + A^{\bar{\bullet}}$ – Charge transfer and separation

The above steps are not necessarily all involved in each particular case. In principle, electron transfer can occur from either singlet or triplet excited state of the donor. As a rule, the acceptor should have a lower-lying empty energy level in comparison to the donor excited state.

In some cases, electron transfer can take place from a ground-state donor to an excited acceptor:

$$D + A^{S_1 or T_1} \rightarrow [D^{\delta+} \ldots A^{\delta-}]^{SorT} \rightarrow [D^{\ddagger\bullet} \ldots A^{\bar{\bullet}}]^{SorT} \rightarrow D^{\ddagger\bullet} + A^{\bar{\bullet}}$$

This can be understood that, as the excitation of acceptor leaves a "vacancy" in its HOMO level, and the vacancy can accommodate an electron from the donor, this will result in a new vacancy in the donor HOMO. Such a vacancy is termed a "hole". The above process can be viewed as a hole being is transferred from the acceptor to the donor, but in this case the HOMO level of the acceptor should be lower than that of the donor.

It is worth noting that an electronic excited state can be seen as a bound electron-hole pair, and its return to ground state can be seen as recombination of the electron and hole. This concept is important to understand the nature of excita-

tions and charge carriers in the solid state (these will be discussed later in the chapter).

Some of the transient states during PIET, for example $[D^{\bullet+} \ldots A^{\bullet-}]^{SorT}$, may lose their energy and return to ground state via nonirradiative relaxation or photon emission. The emission is generally of a low quantum yield because the transition is symmetry-forbidden. An exciplex is actually a stabilized state of $[D^{\delta+} \ldots A^{\delta-}]^{S}$. The complex $[D^{\bullet+} \ldots A^{\bullet-}]^{SorT}$ is generally termed a photoinduced charge-transfer state or simply a charge-transfer (CT) state. When the donor and the acceptor are in the same molecule, this is termed an intramolecular charge-transfer (ICT) state. The formation of a CT or ICT state leads to a quenching of the donor emission. In comparison to the locally excited state (D*), the CT state is of a lower energy and emits at a longer wavelength with a broad, structureless emission band. Moreover, the CT state possesses a larger dipole moment as a result of charge separation. Thus, it generally becomes more stable in a polar medium, and its emission becomes remarkably red-shifted with increasing solvent polarity. One special case of ICT is termed twisted intramolecular charge-transfer (TICT), where the donor and acceptor groups are coplanar and electronically coupled at ground state, but twisted relative to each other and hence are decoupled at ICT state. Such a twisted structure will stabilize the separated charges and cause the TICT process to be more favorable from a thermodynamic aspect.

The separated charges, $D^{\bullet+}$ and $A^{\bullet-}$, can recombine and eventually return to the neutral ground states D and A; this process is termed charge recombination or electron back transfer.

If the PIET occurs from D^{S_1} to A, it leads to quenching of the fluorescence of the donor. The acceptor molecules act as quenchers. Assuming the rate constant of PIET to be k_{ET}, then:

$$\tau_D = 1/(k_f + k_{nr}) \tag{1.7}$$

$$\tau = 1/(k_f + k_{nr} + k_{ET}) \tag{1.8}$$

and thus

$$k_{ET} = \frac{1}{\tau} - \frac{1}{\tau_D} \tag{1.9}$$

This equation provides a simple means of measuring the rate constant of PIET by recording the fluorescence lifetime of the donor in the case that PIET is the major fluorescence quenching pathway. For a more precise measurement, the formation of radical ions or other transient species should be traced, using for example ultrafast spectroscopy methods.

In organic systems, PIET is generally a short-range interaction. In order for electron transfer to occur, the donor and acceptor should be sufficiently close that their molecular orbitals become overlapped. In quantum mechanics theory, this corresponds to a spatial overlap of the donor and acceptor wavefunctions. Long-range electron transfer may take place when the donor and acceptor are linked through a bridge molecule.

The rate of electron transfer reactions including PIET can be interpreted by the Marcus theory [8–18, 20–40]. This theory was originally developed by Rudolph A. Marcus from classical mechanical considerations, though similar expressions were lately derived from a quantum mechanical viewpoint. The Marcus model takes the donor and acceptor together with the surrounding environment (e.g., solvent molecules) as a whole system when considering the nuclei motions in response to electron transfer. The final equation is expressed as:

$$k_{ET} = \frac{2\pi}{h}|H|^2 \frac{1}{\sqrt{4\pi k_B T \lambda}} \exp\left[-\frac{(\Delta G^0 + \lambda)^2}{4\lambda k_B T}\right] \tag{1.10}$$

where k_{ET} is the rate constant for electron transfer, h is the reduced Plank constant, $|H|$is the electronic coupling between the initial and final states, λ is the reorganization energy, ΔG^0 is the total Gibbs free energy change for the electron transfer reaction, k_B is the Boltzmann constant, and T is the absolute temperature. The reorganization energy is defined as the energy required to "reorganize" the system structure from initial to final coordinates, without making the electron transfer (Figure 1.9). The reorganization is a set of vibrational motions of nuclei in the system.

1.3.2.2 **Excitation Energy Transfer**

An excited molecule/chromophore (donor) can transfer the excitation energy to another molecule/chromophore (acceptor) under certain circumstances. The donor molecules typically emit at shorter wavelengths that overlap with the absorption spectrum of the acceptor. If the donor and acceptor are denoted as D and A, respectively, then the process can be expressed as:

$$D^* + A \rightarrow D + A^*$$

where D* and A* are electronic excited states of D and A, respectively. Apparently, the energy transfer will compete with the irradiative decay of D* or, in the other words, it results in a quenching of the fluorescence (or phosphorescence) of the donor. If A* can decay irradiatively, then fluorescence of the acceptor will be observed following excitation of the donor.

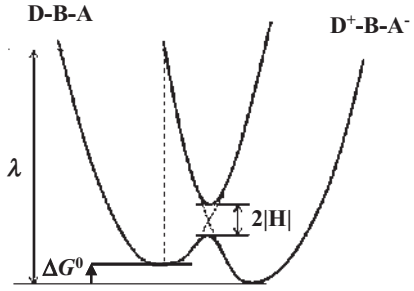

Figure 1.9 Energy potential curve of an electron-transfer reaction.

In the general case, D* and A* are both singlet electronic excited states (S_1), a case that is often termed as singlet–singlet energy transfer. There are other possibilities, however, such as triplet–singlet energy transfer (transfer of excitation from an excited donor in triplet state to produce an excited acceptor in singlet state), and triplet–triplet energy transfer. Energy transfer processes occur typically on time scales that range from picoseconds to nanoseconds for singlet energy transfer up to milliseconds and seconds for triplet energy transfer, because of the much longer lifetimes of triplet states.

Excitation energy transfer between organic molecules is a ubiquitous phenomenon in Nature, a prominent example being the photosynthetic process. In photosynthesis, following photon absorption by light-harvesting complexes, the electronic excitation energy is transferred efficiently towards the photosynthetic reaction center, where the light energy is converted into chemical energy. Energy transfer is also of crucial importance for the application of conjugated materials in organic electronics. For instance, in organic solar cells and photodetectors, the neutral excitations generated by photon absorption must be transferred to particular interfaces in order to dissociate into free charges. In OLEDs, a high-energy gap donor material (host material) is often blended with a low-energy gap acceptor (dopant), so that the singlet and/or triplet excitons created by charge recombination in the host material can be transferred to the dopants, where they are emitted.

Two simple approaches are often used to describe excitation energy transfer in conjugated organic materials, namely the well-known Förster and Dexter models for energy transfer [36].

1.3.2.2.1 The Förster Model

In the framework of Förster theory, energy transfer is mediated via a long-range resonant dipole–dipole interaction between the donor and acceptor molecules. In this case, a chromophore can be roughly seen as a dipole oscillator that is capable of exchanging energy with another dipole having a similar resonance frequency. This is similar to the behavior of coupled oscillators – much like two swings on a common supporting beam [36]. For the above reason, Förster energy transfer is often termed resonance energy transfer or fluorescence resonance energy transfer (FRET). It should be noted that the energy is not actually transferred by fluorescence nor by any other irradiative channel; this case should be distinguished from the situation where the fluorescence of D is reabsorbed by A.

For energy conservation, FRET requires a spectral overlap of the emission spectrum of the donor with the absorption spectrum of the acceptor (Figure 1.10). The extent of energy transfer is then determined by the distance between the donor and acceptor, and the extent of spectral overlap. For convenience, the spectral overlap is described in terms of the Förster radius (R_0). Here, the rate constant of energy transfer k_{DA} is expressed by:

$$k_{DA} = \frac{1}{\tau_D}\left(\frac{R_0}{R}\right)^6 \tag{1.11}$$

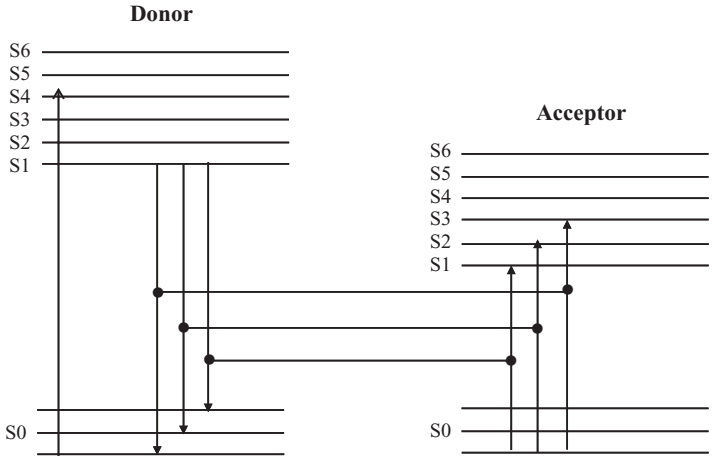

Figure 1.10 Schematic illustration of Förster resonance energy transfer. The donor emission and acceptor absorption should overlap for energy conservation.

where τ_D is the measured fluorescence lifetime of the donor in the absence of the acceptor, and R is the distance between donor and acceptor. If $R = R_0$, the energy transfer rate becomes $k_{DA} = \frac{1}{\tau_D} = k_f + k_{nr}$; that is, the energy transfer has the same rate as the excited state decay expressed by the sum of the rates of radiative and nonradiative pathways. Therefore, the Förster radius R_0 is the distance at which the FRET efficiency of a D–A pair is 50%. At this distance, the donor emission would be decreased to half its intensity in the absence of acceptors. Based on dipole approximation, the Förster radius can be derived as:

$$R_0^6 = \frac{9000(\ln 10)k^2\Phi_D}{128\pi^5 N_A n^4 \tau_D} J \tag{1.12}$$

where Φ_D is the fluorescence quantum yield of the donor in the absence of acceptor, n is the refractive index of the medium, and N_A is Avogadro's number. The term k^2 is a factor describing the relative orientation in space of the transition dipoles of the donor and acceptor. J is the spectral overlap, defined as

$$J = \int F_D(\lambda)\varepsilon_A(\lambda)\lambda^4 d\lambda \tag{1.13}$$

where $F_D(\lambda)$ is the emission intensity of the donor at wavelength λ, being normalized so that $\int F_D(\lambda)\, d\lambda = 1$; $\varepsilon_A(\lambda)$ is the molar extinction coefficient of the acceptor at λ.

FRET is a long-range interaction, and does not require a close contact of the donor and acceptor. For some donor–acceptor pairs, the Förster radius may be up to 10 nm, which is much larger than the general molecular radius.

The distance-dependence of FRET allows the measurement of distances between the donors and acceptors. This principle has been proven to be very useful in

measuring the distances between two sites on a biologically macromolecule (e.g., a protein) by covalently labeling one of the sites with a donor and the other with an acceptor [36]. Similar approaches have been used to study the conformational dynamics of biomolecules.

It should be noted that the simple dipole approximation may break down in situations where the chromophores are in close proximity, or are linked by bridging moieties. Nevertheless, in many instances the Förster approach can provide a useful, and at least qualitatively correct, physical picture for even complex donor–acceptor systems [41].

1.3.2.2.2 **The Dexter Model**

In the Dexter model [42], the energy transfer is similar to a bimolecular reaction, and requires an overlap of the involved donor and acceptor molecular orbitals. Electron exchange can only take place in the overlap region. Because the overlap decays exponentially with distance, it is expected that the rate constant k_{DA} decreases even more rapidly with R than was observed in the case of FRET. In comparison to FRET, Dexter energy transfer is a short-range interaction and occurs typically over distances which are similar to the van der Waals distance – that is, $R = 0.5$–1.0 nm. The rate constant k_{DA} falls exponentially with the distance R between D and A:

$$k_{DA} = KJ \exp(-2R / L) \tag{1.14}$$

where K is a constant in relation to the involved molecular orbitals, J is the spectral overlap between the donor emission and acceptor absorption, and L is the effective average Bohr radius, which is typically on the order of 0.1–0.2 nm.

Dexter energy transfer is a correlated two-electron exchange process. Hence, it allows triplet energy transfer without the additional need for intersystem crossing upon energy transfer of a triplet state. This is in contrast to the Förster energy transfer, which would require a spin-flip for each triplet energy transfer step. For this reason, singlet energy transfer is usually described in the framework of Förster theory, whereas triplet energy transfer is described by the Dexter mechanism [41].

In solution, the donor and acceptor molecules must be close enough for the electron exchange to occur. In this case, the Dexter energy transfer is diffusion-controlled. In contrast, the apparent rate of Förster energy transfer can exceed the diffusion limit. In amorphous films of a donor host doped with a small amount of an acceptor guest, both processes can – in principle – take place, such that the resulting energy transfer mechanism is likely to be a superposition of both modes, depending on the time and distance after the excitation.

In both electron- and energy-transfer cases, the transition mechanism involves vibrational motions driving the reaction coordinates from reactants to products [2]. Therefore, the Marcus model for electron transfer can be implanted into energy transfer cases by considering the energy donor and acceptor and surrounding environment as an entire system.

1.4
Some Basic Concepts of Electronic Process in Conjugated Polymers

In Section 1.3, mention was made of electronic processes in model systems that consisted of only one or two molecules. The situation in the solid state is much more complicated, as the complicity has two aspects: (i) many molecules/atoms interact with each other in a complicated fashion, leading to numerous possible electronic and vibrational states; and (ii) energy and charge transport are typically multistep processes with complex dynamics. In order to describe organic solids, a variety of concepts and terms have been utilized, including energy band, polaron, and exciton, all of which are commonly used in condensed-matter physics. In the following subsections, these basic concepts will be interpreted from a chemist's point of view, with attention focused on conjugated polymers as a representative type of organic semiconductor.

The first step is to provide a brief description of the energy band, which is a very useful concept in solid-state physics. When atoms/molecules are brought together to form a solid, they begin to influence each other. For instance, the outer shell electrons of a molecule will be attracted by the nuclei in other molecules, leading to considerable modifications to their energy levels. This corresponds to a splitting of the atomic/molecular orbitals and a redistribution of the energy levels. For many atoms/molecules, the number of orbitals becomes exceedingly large, and consequently the difference in energy between them becomes very small. Thus, in solids the levels form continuous bands of energy (Figure 1.11) rather than the discrete energy levels of the independent atoms/molecules. Meanwhile, there may be still an energy range left where no electron orbital exists; this is termed the band gap. Typically, an insulator or semiconductor possesses an almost fulfilled band immediately below the band gap, and an almost unoccupied band immediately above the band gap. The former is termed the valence band (VB), and the

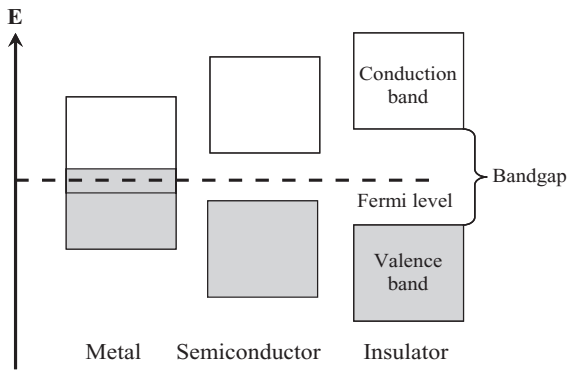

Figure 1.11 Energy band structures of metal, semiconductor, and insulator. The Fermi level is a hypothetical energy level at which an orbital is exactly half-filled.

latter the conduction band (CB). In inorganic semiconductors such as silicon, some of the electrons at the VB may be thermoactivated into the CB, resulting in a small number of mobile "free" electrons in the CB and some mobile holes in the VB. It is for this reason that the materials demonstrate semiconductivity. Whereas, insulators cannot conduct electricity because their band gaps are too large for the thermoexcitation of electrons, metals generally have overlapped VBs and CBs (i.e., no band gap) and thus show good conductivity, even at low temperature.

Traditional polymers such as plastics and rubbers, the backbones of which are mainly composed of saturated carbon atoms linked by single covalent bonds, have good insulating properties. In contrast, conjugated polymers have alternating single and double bonds in their backbones (the molecular structures of some prototype conjugated polymers are shown in Figure 1.1). In the case of t-PA (the simplest conjugated polymer), each carbon atom is connected to one hydrogen atom and to two neighboring carbon atoms through σ bonds. If the carbon–carbon bond lengths were uniform, and there was an unpaired electron on each carbon atom, then the π orbitals would be degenerate and half-filled (Figure 1.12), and the polymer chain would behave like a one-dimensional (1-D) metal. However, this geometry is unstable, and the polymer chain favors a structure with alternating single and double bonds. As a result, the polymer behaves like an insulator rather than a metal. On the other hand, it has been found that charge carriers can be generated in this polymer through chemical reduction/oxidation – that is, by adding electrons into the conjugation system or by taking electrons out [8]. In this way, it has been shown possible to fine-tune the conductivity of t-PA, from insulating to metallic, through redox doping.

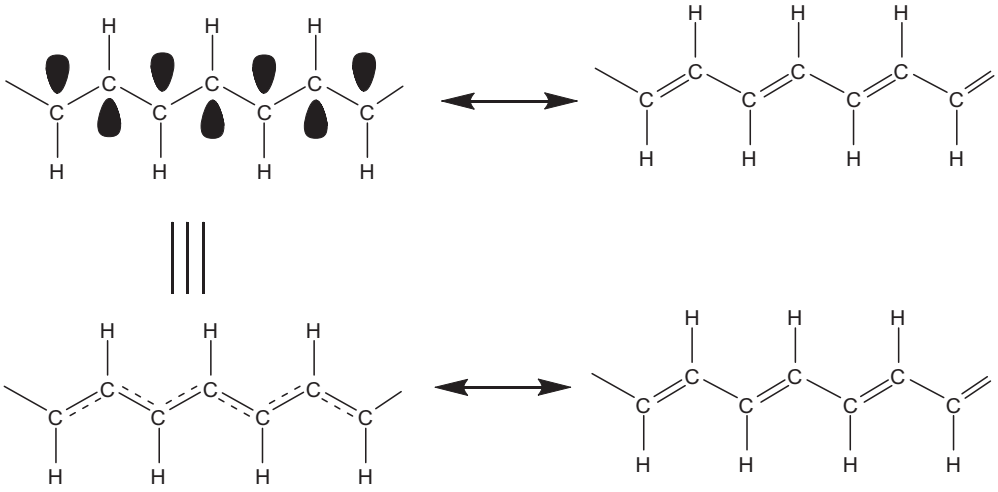

Figure 1.12 Electronic structure of *trans*-polyacetylene: π-orbitals are either half-filled (not stable) or fully filled (stable) forms.

During the 1970s, doping-induced conductivity in conjugated polymers attracted much attention from condensed-matter theorists, and also from chemists and materials scientists. Since the 1980s, however, interest in π-conjugated polymers has been mainly focused on the semiconducting behavior of the pristine systems, rather than on the conducting behavior of the doped materials. While showing much promise in terms of their electronic properties, conjugated polymers can – at least in principle – maintain the good mechanical properties of typical polymers. In fact, conjugated polymer materials have been produced with a conductivity close to that of copper, and with a mechanical performance comparable to that of steel [43]. The development of conjugated polymer-based flexible displays [44] and plastic solar cells [45] has also been demonstrated. Until now, conjugated polymers have shown a wide range of potential, for example in static proofing, radiation protection, corrosion resistance [46], molecular wires and organic circuits [47], lighting and display [48], solar energy conversion and photodetection [49], as well as biological and chemical sensing [16, 50].

1.4.1 Excited States in Conjugated Polymers

There exist various types of charged or neutral excited states (excitations) in conjugated polymers, depending on the molecular structure and the extent of doping. In order to account for their coupling with surrounding environments (lattice distortions), these excited states are generally treated as "qausiparticles" rather than as pure electronic states. This treatment is particularly useful when considering the transport of a charge or an electron-hole pair in a solid. For example, when an electron travels through a solid, its motion is disturbed in complex fashion by its interactions with all other electrons and nuclei; nonetheless, it still behaves (largely) like an electron but with a different mass, traveling unperturbed through free space. This "electron" with a different mass is termed an "electron quasiparticle" (but simply as an electron for convenience). Other terms used include solitons, polarons, bipolarons, and excitons to describe different type of excitations. The chemical nature of these excitations, and their characteristic properties, are described in the following subsections.

1.4.1.1 **Soliton**

Among conjugated polymers, t-PA is unique as it possesses a degenerate ground state – that is, two geometric structures corresponding exactly to the same total energy [51, 52]. The two structures differ one from another by the exchange of carbon–carbon single and double bonds. It was noted above, that every carbon atom in t-PA has one electron in the p_z orbital, and each two electrons form a π-bond. However, for t-PA containing an odd number of carbon atoms, one unpaired electron will remain unpaired such that a radical will occur in the 1-D chain. By chemical redox, this radical can be turned into a positive or negative charge, so that it can act as a boundary between two segments with opposite ground-state geometries (Figure 1.13). In physics terminology, such a radical or charge associ-

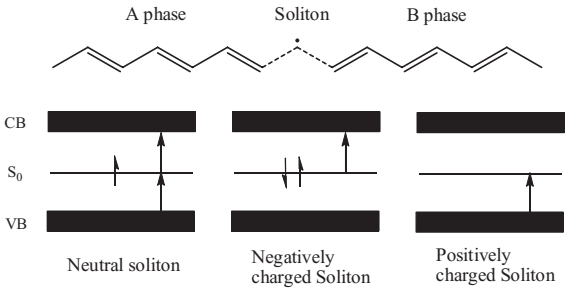

Figure 1.13 Upper: Schematic illustration of a neutral soliton in *trans*-polyacetylene (t-PA); Lower: Band structure for a t-PA chain containing a neutral soliton, a negatively charged soliton, and a positively charged soliton. The allowed transitions are indicated by solid arrows.

ated with a boundary is called a soliton, because it has the properties of a solitary wave that can propagate without deformation and dissipation [51]. The soliton can propagate freely along the polymer chain, as its two sides possess identical energy. In a long chain, the unpaired electron in a neutral soliton (or a charge in a charged soliton) will not be localized on one carbon but rather will be spread over several carbon atoms (up to 14), which causes the soliton to have a width. Although the bond lengths are equal at the middle of the soliton, starting from one side of the soliton the double bonds become gradually longer and the single bonds shorter; consequently, on reaching the other side of the soliton the alteration has completely reversed [51].

The presence of a soliton leads to the appearance of a localized electronic level at mid-gap, which is half-occupied in the case of a neutral soliton and empty (doubly occupied) in the case of positively (negatively) charged soliton (Figure 1.13). Upon increasing the doping level, soliton states at midgap begin to overlap and to form a soliton band. Solitons are one of the primary types of charge carrier in doped t-PA. Solitons only exist in conjugated molecules/polymers with a degenerate ground state; that is, the exchange between the single and double bonds does not alter the total energy of the molecule.

1.4.1.2 **Polaron**

Unlike t-PA, conjugated polymers such as PPP, polypyrrole, and polythiophene possess a nondegenerate ground state, since their ground state corresponds to an aromatic geometry, while the exchange of single bonds with double bonds would result in a quinoid-like structure with a higher total energy [51]. In such polymers, the main charged excitations are radical ions strongly coupled with lattice distortion; these are termed polarons (a positive polaron in the case of a radical cation, and a negative polaron in the case of a radical anion). The net charges in polarons are the result of chemical reduction/oxidation, electrochemical charge injection, or photoinduced charge transfer. The local lattice distortion tends to localize the charge; this corresponds to an upshift of the local HOMO from the valence band,

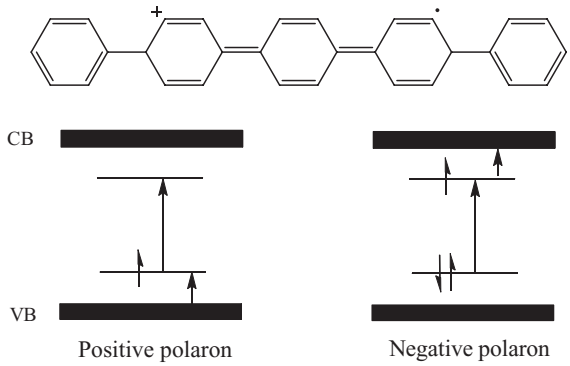

Figure 1.14 Upper: Schematic illustration of a positive polaron in poly(*p*-phenylene) (PPP); Lower: Band structure for a PPP chain containing a positive polaron or a negative polaron. The allowed transitions are indicated by solid arrows.

and a downshift of the LUMO from the conduction band. It should be noted that the valence band remains full and the conduction band remains empty in this case. The geometry of a conjugated polymer PPP in the presence a positive polaron is shown in Figure 1.14. The transition between central anti-symmetric ω_0 and symmetric ω_1 is allowed, but transition from ω_0 to the conduction band is forbidden. Although polarons can propagate along the polymer chain, the propagation length is strongly limited by conjugation interruptions. It is also possible for a polaron to jump from one chain to another if the acceptor chain possesses a similar lattice distortion to the donor (see the Marcus model in Section 1.3). The recombination of a positive polaron with a negative polaron may result in a singlet or triplet excited state. In OLEDs, holes and electrons are injected from opposite sides and recombine in organic semiconductors to form emissive singlet excited states, while triplet states can also be harvested by adding phosphorescent guest molecules.

1.4.1.3 **Bipolaron**

A bipolaron is a pair of charges of the same sign (dual cations or dual anions) that is coupled to lattice distortion. Bipolarons are similar to polarons, but have larger lattice distortions and begin to dominate at a large doping extent or a high charge injection rate. A positive/negative bipolaron can be seen as taking/adding one electron from/to a positive/negative polaron. Two polarons of the same sign can combine to create a bipolaron, the formation of which implies that the energy gained by the interaction with lattice is larger than the Coulombic repulsion between the two charges of same sign confined in the same location [51].

As the lattice relaxation around two charges is stronger than around only one charge, a bipolaron corresponds to a local shift of HOMO and LUMO even further away from the valence band and conduction band, respectively. Unlike polarons, a bipolaron has no half-filled energy level, and only one transition is allowed for

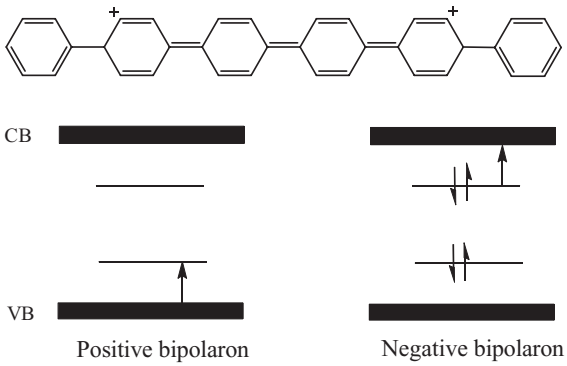

Figure 1.15 Upper: Schematic illustration of a positive bipolaron in PPP; Lower: Band structure for a PPP chain containing a positive bipolaron or a negative bipolaron. The allowed transitions are indicated by solid arrows.

a bipolaron (Figure 1.15). Hence, a bipolaron can easily be distinguished from a polaron by using spectroscopic measurements, such as transient absorption.

1.4.1.4 **Exciton**

The neutral excitations generated following photon absorption or recombination of an electron (negative polaron) and a hole (positive polaron) are termed excitons. These can be regarded as a bound electron–hole pair in a couple with lattice distortion. In general there are three major types of exciton, known as the Frenkel exciton, the Wannier–Mott exciton, and the charge-transfer exciton, respectively. The major differences in these excitons lie in the binding energy between the electron and hole.

- **Frenkel excitons:** These are tightly bound electron–hole pairs, typically with a binding energy of about 1 eV. Due to the strong attraction between the electron and the hole, a Frenkel exciton has a small radius of ~10 . In general, the electron and the hole are located on the same molecule, analogous to molecular excited states (Figure 1.16). Frenkel excitons have well-defined spin states (singlet and triplet), and their transport (diffusion) in solids is generally interpreted by Förster and Dexter energy transfer models.
- **Wannier–Mott excitons:** In comparison to Frenkel excitons, Wannier–Mott excitons possess a much smaller binding energy (typically <0.1 eV), and the electron and hole are only loosely bound in such excitons. In fact, the electron and hole can be treated as two individual quasiparticles (i.e., a negative polaron and a positive polaron) that are bound together by the same lattice distortion. In this sense, Wannier–Mott excitons are also termed neutral bipolarons. A Wannier–Mott exciton has a relatively large radius (~100), while the electron and hole are delocalized (Figure 1.16) and can easily be separated owing to the small Coulombic binding energy. The spin state of Wannier–Mott excitons has

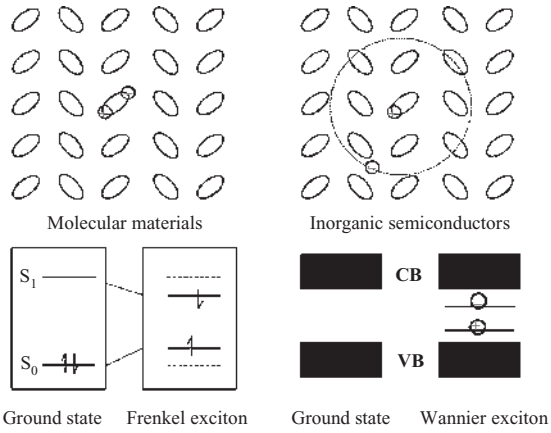

Figure 1.16 Schematic illustration of the difference between a Frenkel exciton and a Wannier exciton.

not been well-defined because of a rapid singlet–triplet exchange. The excitons generated in inorganic semiconductors are usually Wannier–Mott excitons; as these tend to dissociate very rapidly at room temperature they play only a minor role in inorganic semiconductors.

- **Charge transfer excitons:** These are intermediate between Frenkel-type and Wannier–Mott-type excitons. In such excitons, the electron and hole are separated but still tightly bound; the separated charges can be either localized or delocalized in relation to the lattice distortion. Charge transfer excitons are analogous to charge-transfer states observed in D–A molecules. They are often found in charge-transfer crystals, with electrons lying on one of the components and holes on the other component. On the other hand, they may also be formed in solids consisting of only one organic compound.

During recent years there has been much debate concerning the nature of the primary excitations in intrinsic conjugated polymers [53, 54], the main question being whether they are Frenkel excitons, Wannier excitons, charge polarons, or something else? The answer to this point is of crucial importance for the applications of these materials. For example, if the primary excitations are tightly bound excitons, then in electroluminescence devices the injected electron and hole can form a triplet with a spin multiplicity of three, or a singlet with a spin multiplicity of one. Only the latter (corresponding to a formation probability of 25%) will recombine radiatively, unless a triplet-harvesting mechanism is applied. In contrast, with charge polarons as the primary excitations the theoretical maximum efficiency can approach unity. In photovoltaic devices, Frenkel excitons need to diffuse to an interface with built-in electric field (e.g., electron donor–acceptor interface) in order to dissociate into free charges, whereas Wannier–Mott excitons tend to dissociate very rapidly and hence generate free charge carriers locally. In

order to determine the nature of the primary excitations, one key parameter is the binding energy between the electron and hole, and that the solution to the problem is clear for several types of conjugated polymer but ambiguous for some others. Polydiacetylenes, for instance, are believed to have an exciton binding energy of about 0.5 eV according to photoconductivity spectrum and electroabsorption measurements [53]. For PPV and its soluble derivatives, however, it has been reported that photoconductivity began to appear at the onset of optical absorption, implying a bind energy <0.1 eV. Yet, a value of ~0.4 eV was derived from other experimental approaches, such as photovoltaic working spectrum, electric field-induced photoluminescence quenching, and magnetic field dependence of photoconductivity. Currently, it is more widely accepted that the lowest energy excitations in conjugated polymers are neutral Frenkel excitons.

The delocalization degree of an exciton in conjugated polymers is prevailingly determined by the conjugation lengths of the segments. As noted above, the effective conjugation length is greatly limited by the chemical and physical defects in the polymer backbone. The most commonly discussed defects include saturated carbon atoms, *cis*-isomerization kinks, and bending and twisting of the backbone. Such defects are unavoidable as they are brought to the polymer chains during material synthesis and processing, and even if an ideal chain without chemical defects could be obtained, physical defects such as twisting and bending would still be present. It has been claimed that the average conjugation length in PPVs is only about 10 repeating units [23], and that a conjugated polymer chain can therefore be viewed as consisting of a series of conjugation segments of different lengths (Figure 1.17). These conjugation segments are generally treated as weakly

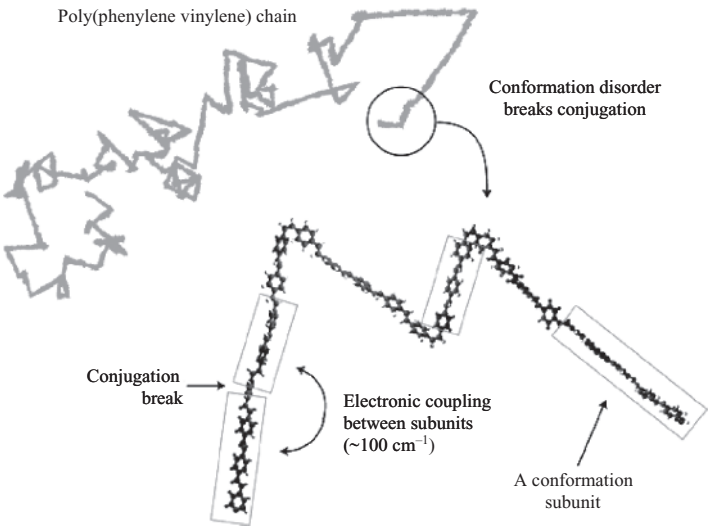

Figure 1.17 Schematic illustration of a PPV chain with defects. Reproduced with permission from Ref. [55]; © 2006, Nature Publishing Group.

coupled chromophores where, typically, shorter segments have absorption and emission in the bluer range, and longer in the redder range. Excitons that are generated on relatively short segments tend to migrate to relatively long segments via for example, resonance dipole coupling or electron exchange. A general belief here is that a migration process consists of a succession of energy-transfer steps, and that the transfer direction of each step obeys the probability law. This is known as the "random-walk model" [56] of energy migration; such a migration process is also referred to as exciton diffusion, as it is similar to the diffusion motion of a molecule/particle in solution.

1.4.2 Interactions between Conjugated Polymer Chains

In the solid state of conjugated polymers, there often exists a strong interchain π–π stacking interaction, especially when the conjugated backbones have a rigid planar structure. Intrachain π–π stacking may also be present in self-folded polymer chains, with two or more adjacent conjugated polymer chains or chain segments forming excimers or interchain/intersegment charge-transfer states as a result of the overlapping of π-orbitals. It should be noted that the degree of chain stacking depends significantly on the way in which the polymer is processed to form the film [57]. Interchain interactions can be evaluated experimentally by comparing the optical spectra of pristine films with those of diluted films (i.e., blends with an inert polymer matrix, such as polystyrene) and solutions. As a replacement for the pristine film, nanosized aggregates of conjugated polymers can be prepared artificially by a controlled precipitation in a poor solvent [58]. The formation of interchain excitations results in a quenching of fluorescence and the appearance of emission bands at longer wavelength regions. Hence, the fluorescence quantum yields of the conjugated polymers in dilute solutions and diluted films are generally larger than those measured in dense films and aggregates. In fact, aggregation-induced fluorescence quenching is a common phenomenon for organic conjugated molecules, although there are some exceptions, with aggregation-induced emission enhancement having been reported in some systems [59–61]. The enhancement mechanisms were generally explained as a suppression of the nonirradiative decay channels of the excited states; for example, decay via a molecular rotational relaxation can be diminished upon aggregation, due to the strong intermolecular steric repulsions.

The interchain excitations reported in conjugated polymers can be categorized as three major types, namely bound polaron pairs, excimers, and ground-state complexes.

1.4.2.1 **Bound Polaron Pairs**

The first evidence of bound polaron pairs in conjugated polymers was reported by Rothberg *et al.* during the 1990s [62–64]. On investigating the fluorescence of PPV and poly(2-methoxy,5-(2′-ethylhexoxy)-4-phenylenevinylene (MEH-PPV) films at selected excitation wavelengths (300 nm and 500 nm), Rothberg's group showed

that the fluorescence quantum yield was lower at a shorter excitation wavelength, but that the emission spectrum and the fluorescence lifetime were maintained in a similar state. These observations indicated that not all of the photons absorbed by PPV would result in singlet excitons, especially at a shorter excitation wavelength (i.e., a higher photon energy). More recently, the same group conducted picosecond transient absorption experiments on PPV, and showed that the generation efficiency of singlet excitons could be much smaller than unity. A transient species that was unrelated to the emission pathway was also observed, but this could not be assigned as either singlet or triplet excitons, nor polarons or bipolarons. Ultimately, the conclusion was reached that bound polaron pair formation was a prominent photophysical pathway in PPV films. Bound polaron pairs, by definition, are Coulombic bound charges on adjacent chains that are formed by the dissociation of hot intrachain singlet excitons (a "hot exciton" is an exciton away from thermodynamic equilibrium state) on a subpicosecond timescale and recombine geminately. It can be seen that bound polaron pairs are essentially charge-transfer excitons. According to Rothberg's interpretations, bound polaron pairs have a lower energy than intrachain singlets at most locations in the polymer, and are basically nonirradiative due to the poor overlapping of wavefunctions of the separated charges. The experimental results of Rothberg showed the generation yield of singlet exciton in PPV to be only about 10%, while 90% of the absorbed photons generated bound polaron pairs [62]. However, this deduction was not supported by follow-up experiments conducted by other groups [65–67], and this in turn led to the conclusion that only a small amount of bound polar pairs was formed in PPV. Moreover, it was also suggested that such a discrepancy had stemmed from the different qualities of PPV samples used, and that the situation was different for the various types of conjugated polymer. For example, according to Sheng *et al.* [67], only about 70% of the photoexcitations in polythiophene are singlet excitons, whereas the other 30% are most likely polarons or polaron pairs; in the case of PPV, the singlet exciton generation yield is close to unity.

1.4.2.2 **Excimers**

Excimer formation in conjugated polymers was studied systematically by Jenekhe *et al.* during the 1990s [68, 69]. Similar to the formation of excimers in small molecules, an excimer in conjugated polymers is generated by an excited chain and a neighboring chain in the ground state. The two chains should have a short interchain distance (0.3–0.6 nm) for efficient π-orbital overlapping. It is possible to have more chains (conjugated segments) involved in excimer formation; that is, the charge density (electron wavefunction) can be distributed over more than two chains. However, in comparison to bound polaron pairs, the extent of charge separation is much smaller in excimers, where the electrons and holes are still tightly bound. Hence, excimers are essentially Frenkel excitons, and are slightly delocalized as a result of a weak intermolecular electronic coupling. When compared to intrachain Frenkel excitons, the emission of the excimer lies in a relatively long wavelength range (see the orbital splitting model in Figure 1.7). It should be

borne in mind that an excimer will dissociate when it returns to the ground state, but that any transition between the ground state and excimer state is symmetry-forbidden. Consequently, excimer formation will have no effect on the UV-visible absorption spectrum of a conjugated polymer. For the same reason, excimers possess a lower irradiation rate and a longer lifetime than intrachain excitons.

1.4.2.3 Ground-State Complexes

Similar to the formation of an excimer, molecular orbital splitting will occur if two or more ground-state molecules come sufficiently close together that their inner shell molecular orbitals begin to overlap. The thus-formed ground-state complex has an excited state which may be either an interchain Frenkel exciton or a charge-transfer exciton (bound polaron pair), depending on the degree of charge separation. Due to orbital splitting, the energy gap between the ground state and excited state becomes smaller; consequently, ground-state complexes typically show a red-shifted absorption and red-shifted emission spectra compared to free chromophores. Ground-state complexes are similar to excimers with regards to their emission properties. For example, they both show weak, low-energy, broad and structureless emission bands and a relatively long fluorescence lifetime. The absorption spectral change allows a distinction to be made between ground-state complexes and excimers. It has been proven experimentally that these complexes can be formed in some conjugated polymers [70–74]. The fluorescence spectra of MEH-PPV in films and different solvents are shown in Figure 1.18, where the broad red-shifted bands observed in MEH-PPV films could be assigned to ground-state complexes and excimers. Another good example is a ladder-type conjugated polymer MLPPP (see Figure 1.1), the backbone of which is constituted by fused fluorene rings. MLPPP is planar and highly rigid, so that the polymer chains may be easily arranged in a parallel, face-to-face manner in the solid state. Moreover, the π–π stacking interactions are so strong that ground-state complexes are formed, as proven by the observation of low-energy absorption and emission bands in solid films of MLPPP [70]. As such low-energy bands cannot be observed in dilute solutions, these must have derived from interchain interactions. A similar phenomenon was observed with poly(5-(pyridin-2-yl)vinylene), a heteroatom polymeric derivative of PPV where, in comparison to the phenyl rings in PPV, the pyridine groups have a higher electronegativity that promotes interchain coupling [75].

1.4.3 Photoinduced Charge Transfer between Conjugated Polymers and Electron Acceptors

Photoinduced charge transfer can occur when a conjugated polymer is blended with an electron acceptor. The radical cations (positive polarons) produced are stabilized by the conjugated polymer backbone as the result of a delocalization of charge density over the conjugation units. The energy diagram for photoinduced charge transfer between a conjugated polymer and an electron acceptor is depicted in Figure 1.19.

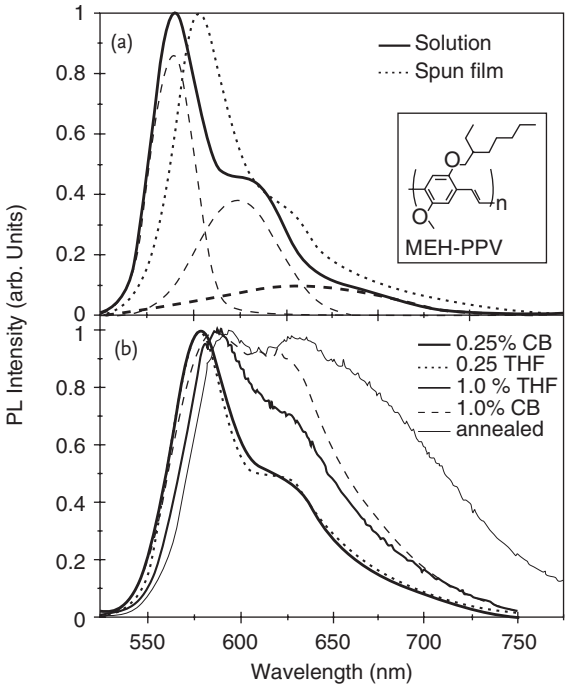

Figure 1.18 Normalized photoluminescence (PL) spectra of MEH-PPV in different environments. (a) PL spectra of a 0.25% (w/v) solution of MEH-PPV in chlorobenzene (CB) (solid curve), and the film resulting from spin-casting the solution (dotted curve). The small dashed curves show Gaussian fits to the three visible peaks of the solution PL; (b) PL spectra of MEH-PPV films cast from a 0.25% (w/v) solution in CB [solid curve, same as dashed curve in panel (a)], a 0.25% (w/v) solution in tetrahydrofuran (THF) (dotted curve), a 1.0% solution in THF (gray solid curve), a 1.0% solution in CB (dashed curve), and the film cast from the 1.0% CB solution after annealing (thin solid curve). Reproduced with permission from Ref. [74]; © 2000, American Chemical Society.

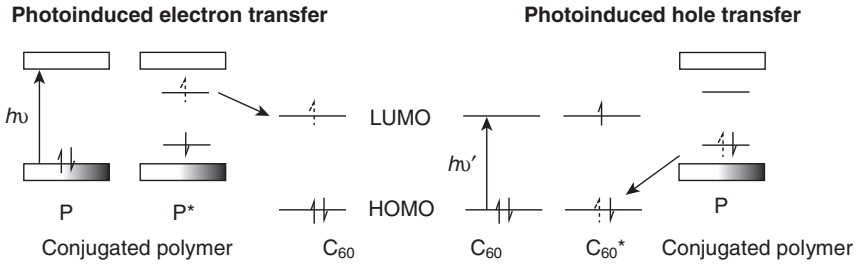

Figure 1.19 Energy diagram illustration of photoinduced charge transfer between conjugated polymer and acceptor (C_{60}). The electron being transferred is depicted as a dashed arrow.

Fullerene (C_{60}) and its derivatives are good electron acceptors, and promising photovoltaic effects in a blend film of MEH-PPV and C_{60} were first described by Sariciftci *et al.* in 1992 [76]. These findings aroused much interest in the development of conjugated polymer-based solar cells that could be used to convert solar energy into electricity. The primary structure of an organic solar cell includes an active layer (the donor–acceptor blend film) that is sandwiched between a transparent conductive anode [e.g., indium tin oxide (ITO) glass] and a metal cathode. Since the early 1990s, major progress has been made in this field, notably in 1995 by Yu *et al.*, who achieved an energy conversion efficiency of 3% by controlling the morphology of the blend film of MEH-PPV and C_{60} to form an interpenetrating network structure [77] (further details are available in Chapter 9). At this point, mention must be made of some of the important steps in energy conversion processes [2].

In organic solar cells, the main steps are as follows.

1) **Light harvesting:** Light is absorbed in the blend film and generates singlet excitons; for solar cells, the absorption should match the solar spectrum as closely as possible.

2) **Exciton diffusion and charge separation:** Excitons must migrate towards the D–A interfaces (heterojunctions); for interpenetrating structures, many local interfaces exist. At the D–A interface, excitons can dissociate into separated charges as a result of electron-transfer processes between the donor and the acceptor; the exciton diffusion length in typical conjugated polymers is about 5 nm, and in the ideal case the heterojunctions should be arranged in such a way that every exciton can locate a heterojunction during its lifetime.

3) **Charge transport:** The separated charges drift in the organic layers, under the driving force of the built-in electric field between the two electrodes.

4) **Charge collection:** The charges must ultimately be collected at the electrodes.

Of the above steps, charge separation is central. As noted in the earliest study on MEH-PPV/C_{60} systems [76], no ground-state complex was formed between the polymer and acceptor, as the electronic absorption spectrum of the blend was simply a superposition of the two components. Moreover, the fluorescence of MEH-PPV was heavily quenched by C_{60}, a very small amount of which quenched such fluorescence by three orders of magnitude. In the meantime, the fluorescence lifetime was decreased from 550 ps to far below 60 ps, indicating an electron transfer rate on the order of $10^{12}\,s^{-1}$ (see Eq. (1.9) for the calculation). This rate was much larger than those of the competing irradiative and nonirradiative processes, and suggested a charge-separation efficiency close to unity. More recently, the formation of charge-separation species was further confirmed by measuring the photoinduced transient absorption spectra and light-induced electron spin resonance (LESR) of the blends [78]. Subsequent ultrafast spectroscopic measurements confirmed that the PIET between MEH-PPV and fullerene occurred at a timescale

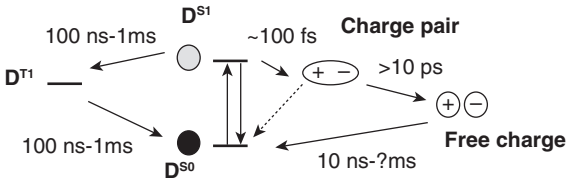

Figure 1.20 Schematic illustration of the photoinduced charge transfer process in conjugated polymer solar cells. Typical time scales for several of the involved steps are also shown.

of ~100 fs [79], which was so rapid that it could even compete with the vibrational relaxation process of the excited states.

Several plausible steps during the photoinduced charge separation process in conjugated polymer/acceptor blends are shown in Figure 1.20; the typical time scales of some steps are also shown. As the efficiency of the charge transfer step is close to unity, the energy conversion efficiency is mainly limited by other processes such as exciton diffusion, charge transport, or charge collection. It should be noted here that charge recombination is an important competing pathway of charge transport.

1.5
Carriers Generation and Transport

The above-described charge carriers (solitons, polarons, bipolarons) exist not only in conjugated polymers but also in other types of organic (semi)conductor. It must be borne in mind that the real charge-carrying particles which can be transported in organic solids are simply electrons. For example, although a polaron is intrinsically a radical ion, its transport is not a translational motion of the entire radical ion but rather is a drift of one electron from the radical ion to another location, where it creates a new radical ion. In this sense, charge transport can be seen as a sequence of redox reactions. From a mathematical aspect, however, it is more convenient and practical to describe the process by using the term "charge carriers."

1.5.1
Charge Carriers

Charge carriers can be generated via optical excitation, electrochemical doping (charge injection from electrodes), or chemical reduction/oxidation reactions. The generation of charge carriers is a precondition for electricity conduction. Taking photoconductors as an example, the main steps include: (i) the generation of conjugated molecules that absorb light and excitons; (ii) the dissociation of excitons into separate charges under the driving force of an external electric field; and

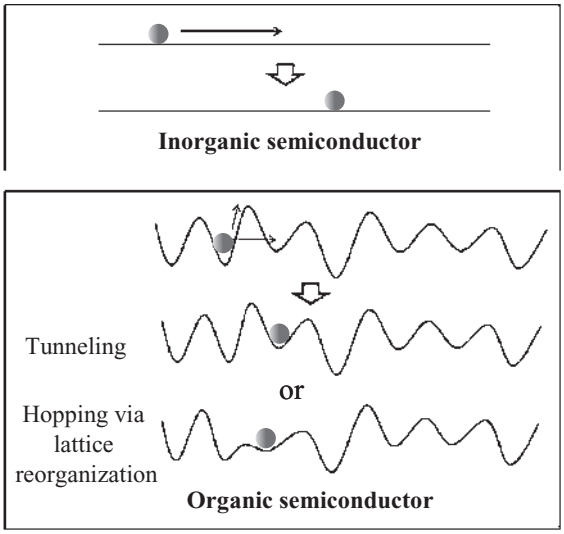

Figure 1.21 Schematic illustration of the transport of a charge carrier (solid ball) in inorganic semiconductors and organic semiconductors. For inorganic semiconductor the energy potential surface is represented as horizontal lines because of negligible energy barriers.

(iii) the generation of a photocurrent as a result of charge transport towards opposite electrodes.

In blending systems consisting of electron donors and acceptors, the charge carrier generation step is often very rapid (100~1000 fs), and its efficiency can approach unity. However, the transport of charge carriers in organic solids is less efficient than in inorganic semiconductors, mainly because charge carriers in organic solids lie within discrete energy levels rather than in continuous energy bands. Likewise, holes and electrons tend to be localized over small regions rather than be delocalized over the entire lattice, as is the case with inorganic semiconductors. Charge transport can only take place through electron hopping or electron tunneling, and it is these processes which essentially determine carrier mobility in organic solids. The energy potential surface for charge transport in inorganic semiconductors and organic semiconductors is illustrated in Figure 1.21.

1.5.2
Carrier Mobility and Its Measurement

The application of an external electric field induces a drift of the charge carriers; the mobility can then be defined as the ratio between the velocity, v, of the charges and the amplitude of the applied electric field, F:

$$\mu = v / F \tag{1.15}$$

The carrier mobility is usually expressed in $cm^2/(V \cdot s)$. *Carrier diffusion* should be seen as a local displacement of the charge around an average position, while drift induces a displacement of the average position. *Drift* is the effect that dominates the migration of the charges across an organic layer in the devices.

Charge mobilities can be determined experimentally by applying various techniques [21], one of the simplest of which is termed time-of-flight (TOF). In this technique, a thin organic layer (of a few microns thickness) is sandwiched between two electrodes, one of which is transparent (e.g., ITO glass). The material to be tested is first irradiated by a laser pulse in the proximity of the transparent electrode, in order to generate charges. Depending on the polarity of the applied bias and the corresponding electric field (in the range of 10^4 to $10^6\,V\,cm^{-1}$), the photogenerated holes or electrons migrate across the material towards the other electrode. The current at that electrode is recorded as a function of time, and the mobility of the holes or electrons is then estimated via:

$$\mu = \frac{v}{F} = \frac{d}{Ft} = \frac{d^2}{vt} \tag{1.16}$$

where d is the distance between the electrodes, F is the electric field, t is the averaged transient time, and V is the applied voltage. For ordered materials a sharp onset will be obtained, whereas for disordered systems such as polymers a broadening of the signal occurs due to a distribution of transient times across the material.

Carrier mobilities can also be extracted from current/current density–voltage curves measured in a FET or a photovoltaic diode. In another technique, termed pulse-radiolysis time-resolved microwave conductivity (PR-TRMC), a pulse of highly energetic electrons is applied to create a low density of free carriers. The carrier mobility can then be derived by recording the pulse-induced change in electrical conductivity as a function of microwave power (further details are available in Ref. [21]).

1.5.3
Mobility-Influencing Factors

An efficient charge transport requires that the charges are able to move from molecule to molecule, and not be trapped or scattered. Therefore, charge carrier mobilities are influenced by many factors that include molecular packing, disorder, and the presence of impurities, temperature, electric field, charge-carrier density, size/molecular weight, and pressure [21]. Moreover, different measuring methods may produce different results, with data derived from methods that measure mobilities over macroscopic distances (~1 mm) often being dependent on the purity and order in the material. Methods that measure mobilities over microscopic distances are less dependent on these characteristics.

Due to the weak intermolecular electronic coupling, the charge carriers must face relatively large energy barriers at the molecular boundaries. Hence, the relative positons (molecular packing) of the interacting molecules are an important

influencing factor for carrier mobility. In most instances, unsubstituted conjugated molecules crystallize into a layered herringbone packing, which gives rise to two-dimensional transport within the stacked organic layers, but transport between the layers is less efficient. Static and dynamic disorders in organic solids also greatly impact on the carrier mobilities, because they introduce spatial and temporal variations to intermolecular coupling strength. More recently, attention has also been paid to other influencing factors, such as temperature and pressure (further details of these issues are discussed in Ref. [21]).

References

1 Markus, S. and Hans, C.W. (2007) *Organic Molecular Solids*, Wiley-VCH Verlag GmbH & Co. KGaA, Weinheim.

2 Brédas, J.-L., Beljonne, D., Coropceanu, V., and Cornil, J. (2004) Charge-transfer and energy-transfer processes in pi-conjugated oligomers and polymers: a molecular picture. *Chem. Rev.*, **104** (11), 4971–5003.

3 Koenigsberger, J. and Schilling, K. (1910) On electrical conductivity in fixes elements and compounds I. Minimum resistance, testing on electron behaviour, use of dissociation formulae. *Ann. Phys.*, **32** (6), 179–230.

4 Volmer, M. (1913) The different photoelectrical occurrences on anthracene, their connections to each other, to fluorescence and dianthracene formation. *Ann. Phys.*, **40** (4), 775–796.

5 Naarmann, H. (2000) Polymers, Electrically Conducting, in Ullmann's Encyclopedia of Industrial Chemistry, Wiley-VCH Verlag GmbH & Co. KGaA, Weinheim.

6 Helfrich, W. and Schneider, W.G. (1965) Recombination radiation in anthracene crystals. *Phys. Rev. Lett.*, **14** (7), 229–231.

7 Pope, M., Magnante, P., and Kallmann, H.P. (1963) Electroluminescence in organic crystals. *J. Chem. Phys.*, **38** (8), 2042–2043.

8 Chiang, C.K., Fincher, C.R., Park, Y.W., Jr, Heeger, A.J., Shirakawa, H., Louis, E.J., Gau, S.C., and MacDiarmid, A.G. (1977) Electrical-conductivity in doped polyacetylene. *Phys. Rev. Lett.*, **39** (17), 1098–1101.

9 Tang, C.W. and VanSlyke, S.A. (1987) Organic electroluminescent diodes. *Appl. Phys. Lett.*, **51** (12), 913–915.

10 Burroughes, J.H., Bradley, D.D.C., Brown, A.R., Marks, R.N., Mackay, K., Friend, R.H., Burns, P.L., and Holmes, A.B. (1990) Light-emitting-diodes based on conjugated polymers. *Nature*, **347** (6293), 539–541.

11 Günes, S., Neugebauer, H., and Sariciftci, N.S. (2007) Conjugated polymer-based organic solar cells. *Chem. Rev.*, **107** (4), 1324–1338.

12 Peumans, P., Yakimov, A., and Forrest, S.R. (2003) Small molecular weight organic thin-film photodetectors and solar cells. *J. Appl. Phys.*, **93** (7), 3693–3723.

13 Dodabalapur, A., Torsi, L., and Katz, H.E. (1995) Organic transistors: two-dimensional transport and improved electrical characteristics. *Science*, **268** (5208), 270–271.

14 Horowitz, G. (1998) Organic field-effect transistors. *Adv. Mater.*, **10** (5), 365–377.

15 Bartic, C., Campitelli, A., and Borghs, S. (2003) Field-effect detection of chemical species with hybrid organic/inorganic transistors. *Appl. Phys. Lett.*, **82** (3), 475–477.

16 Thomas, S.W., Joly, G.D., and Swager, T.M. (2007) Chemical sensors based on amplifying fluorescent conjugated polymers. *Chem. Rev.*, **107** (4), 1339–1386.

17 Berggren, M., Dodabalapur, A., Slusher, R.E., and Bao, Z. (1997) Light amplification in organic thin films using

cascade energy transfer. *Nature*, **389** (6650), 466–469.
18 McGehee, M.D. and Heeger, A.J. (2000) Semiconducting (conjugated) polymers as materials for solid-state lasers. *Adv. Mater.*, **12** (22), 1655–1668.
19 Brütting, W. (2005) *Physics of Organic Semiconductors*, Wiley-VCH Verlag GmbH & Co. KGaA, Weinheim.
20 Agranovich, V. (2008) *Excitations in Organic Solids*, Oxford Scientific Publications, Oxford.
21 Coropceanu, V., Cornil, J., da Silva Filho, D.A., Olivier, Y., Silbey, R., and Brédas, J.-L. (2007) Charge transport in organic semiconductors. *Chem. Rev.*, **107** (4), 926–952.
22 Vardeny, Z.V. (2009) *Ultrafast Dynamics and Laser Action of Organic Semiconductors*, CRC Press, Boca Raton.
23 Mukamel, S., Tretiak, S., Wagersreiter, T., and Chernyak, V. (1997) Electronic coherence and collective optical excitations of conjugated molecules. *Science*, **277** (5327), 781–787.
24 Anthony, J.E. (2006) Functionalized acenes and heteroacenes for organic electronics. *Chem. Rev.*, **106** (12), 5028–5048.
25 Kondakov, D.Y., Pawlik, T.D., Hatwar, T.K., and Spindler, J.P. (2009) Triplet annihilation exceeding spin statistical limit in highly efficient fluorescent organic light-emitting diodes. *J. Appl. Phys.*, **106** (12), 124510.
26 Scherf, U. and List, E.J.W. (2002) Semiconducting polyfluorenes – towards reliable structure-property relationships. *Adv. Mater.*, **14** (7), 477–487.
27 van Nostrum, C.F., Picken, S.J., Schouten, A.-J., and Nolte, R.J.M. (1995) Synthesis and supramolecular chemistry of novel liquid crystalline crown ether-substituted phthalocyanines: toward molecular wires and molecular ionoelectronics. *J. Am. Chem. Soc.*, **117** (40), 9957–9965.
28 Holten, D., Bocian, D.F., and Lindsey, J.S. (2002) Probing electronic communication in covalently linked multiporphyrin arrays. A guide to the rational design of molecular photonic devices. *Acc. Chem. Res.*, **35** (1), 57–69.
29 Tsuboyama, A., Iwawaki, H., Furugori, M., Mukaide, T., Kamatani, J., Igawa, S., Moriyama, T., Miura, S., Takiguchi, T., Okada, S., Hoshino, M., and Ueno, K. (2003) Homoleptic cyclometalated iridium complexes with highly efficient red phosphorescence and application to organic light-emitting diode. *J. Am. Chem. Soc.*, **125** (42), 12971–12979.
30 Evans, R.C., Douglas, P., and Winscom, C.J. (2006) Coordination complexes exhibiting room-temperature phosphorescence: evaluation of their suitability as triplet emitters in organic light emitting diodes. *Coord. Chem. Rev.*, **250** (15-16), 2093–2126.
31 Setayesh, S., Grimsdale, A.C., Weil, T., Enkelmann, V., Müllen, K., Meghdadi, F., List, E.J.W., and Leising, G. (2001) Polyfluorenes with polyphenylene dendron side chains: toward non-aggregating, light-emitting polymers. *J. Am. Chem. Soc.*, **123** (5), 946–953.
32 Sun, Y.M., Xiao, K., Liu, Y.Q., Wang, J.L., Pei, J., Yu, G., and Zhu, D.B. (2005) Oligothiophene-functionalized truxene: star-shaped compounds for organic field-effect transistors. *Adv. Funct. Mater.*, **15** (5), 818–822.
33 Burn, P.L., Lo, S.C., and Samuel, I.D.W. (2007) The development of light-emitting dendrimers for displays. *Adv. Mater.*, **19** (13), 1675–1688.
34 Tao, X.-T., Zhang, Y.-D., Wada, T., Sasabe, H., Suzuki, H., Watanabe, T., and Miyata, S. (1998) Hyperbranched polymers for electroluminescence applications. *Adv. Mater.*, **10** (3), 226–230.
35 Katsis, D., Geng, Y.H., Ou, J.J., Culligan, S.W., Trajkovska, A., Chen, S.H., and Rothberg, L.J. (2002) Spiro-linked ter-, penta-, and heptafluorenes as novel amorphous materials for blue light emission. *Chem. Mater.*, **14** (3), 1332–1339.
36 Lakowicz, J.R. (2006) *Principles of Fluorescence Spectroscopy*, Plenum Press, New York, London.
37 Forster, T. (1969) Excimers. *Angew. Chem. Int. Ed. Engl.*, **8** (5), 333–343.
38 Weller, A. (1982) Photoinduced electron transfer in solution: exciplex and radical

ion pair formation free enthalpies and their solvent dependence. *Z. Phys. Chem.*, **133** (1), 93–98.
39 Marcus, R.A. (1956) On the theory of oxidation-reduction reactions involving electron transfer. I. *J. Chem. Phys.*, **24** (5), 966–978.
40 Marcus, R.A. (1993) Electron-transfer reactions in chemistry. Theory and experiment. *Rev. Mod. Phys.*, **65** (3), 599–610.
41 Laquai, F., Park, Y.-S., Kim, J.-J., and Basché, T. (2009) Excitation energy transfer in organic materials: from fundamentals to optoelectronic devices. *Macromol. Rapid Commun.*, **30** (14), 1203–1231.
42 Dexter, D.L. (1953) A theory of sensitized luminescence in solids. *J. Chem. Phys.*, **21** (5), 836–850.
43 Akagi, K., Suezaki, M., Shirakawa, H., Kyotani, H., Shimomura, M., and Tanabe, Y. (1989) Synthesis of polyacetylene films with high-density and high mechanical strength. *Synth. Met.*, **28** (3), D1–D10.
44 He, Y. and Kanicki, J. (2000) High-efficiency organic polymer light-emitting heterostructure devices on flexible plastic substrates. *Appl. Phys. Lett.*, **76** (6), 661–663.
45 Al-Ibrahim, M., Roth, H.K., Zhokhavets, U., Gobsch, G., and Sensfuss, S. (2005) Flexible large area polymer solar cells based on poly(3-hexylthiophene)/fullerene. *Sol. Energy Mater. Sol. Cells*, **85** (1), 13–20.
46 Kinlen, P.J., Silverman, D.C., and Jeffreys, C.R. (1997) Corrosion protection using polyaniline coating formulations. *Synth. Met.*, **85** (1–3), 1327–1332.
47 Sirringhaus, H., Kawase, T., Friend, R.H., Shimoda, T., Inbasekaran, M., Wu, W., and Woo, E.P. (2000) High-resolution inkjet printing of all-polymer transistor circuits. *Science*, **290** (5499), 2123–2126.
48 Sheats, J.R., Antoniadis, H., Hueschen, M., Leonard, W., Miller, J., Moon, R., Roitman, D., and Stocking, A. (1996) Organic electroluminescent devices. *Science*, **273** (5277), 884–888.
49 Brabec, C.J., Sariciftci, N.S., and Hummelen, J.C. (2001) Plastic solar cells. *Adv. Funct. Mater.*, **11** (1), 15–26.
50 McQuade, D.T., Pullen, A.E., and Swager, T.M. (2000) Conjugated polymer-based chemical sensors. *Chem. Rev.*, **100** (7), 2537–2574.
51 Bredas, J.L. and Street, G.B. (1985) Polarons, bipolarons, and solitons in conducting polymers. *Acc. Chem. Res.*, **18** (10), 309–315.
52 Heeger, A.J., Kivelson, S., Schrieffer, J.R., and Su, W.-P. (1988) Solitons in conducting polymers. *Rev. Mod. Phys.*, **60** (3), 781–850.
53 Sariciftci, N.S. (1998) *Primary Photoexcitations in Conjugated Polymers: Molecular Exciton versus Semiconductor Band Model*, World Scientific, Singapore.
54 Rauscher, U., Bässler, H., Bradley, D.D.C., and Hennecke, M. (1990) Exciton versus band description of the absorption and luminescence spectra in poly(para-phenylenevinylene). *Phys. Rev. B*, **42** (16), 9830–9836.
55 Scholes, G.D. and Rumbles, G. (2006) Excitons in nanoscale systems. *Nat. Mater.*, **5** (9), 683–696.
56 Heun, S., Mahrt, R.F., Greiner, A., Lemmer, U., Bassler, H., Halliday, D.A., Bradley, D.D.C., Burn, P.L., and Holmes, A.B. (1993) Conformational effects in poly(*p*-phenylene vinylene)s revealed by low-temperature site-selective fluorescence. *J. Phys. Condens. Matter*, **5** (2), 247–260.
57 Nguyen, T.Q., Doan, V., and Schwartz, B.J. (1999) Conjugated polymer aggregates in solution: control of interchain interactions. *J. Chem. Phys.*, **110** (8), 4068–4078.
58 Collison, C.J., Rothberg, L.J., Treemaneekarn, V., and Li, Y. (2001) Conformational effects on the photophysics of conjugated polymers: a two species model for MEH-PPV spectroscopy and dynamics. *Macromolecules*, **34** (7), 2346–2352.
59 Luo, J., Xie, Z., Lam, J.W.Y., Cheng, L., Chen, H., Qiu, C., Kwok, H.S., Zhan, X., Liu, Y., Zhu, D., and Tang, B.Z. (2001) Aggregation-induced emission of 1-methyl-1,2,3,4,5-pentaphenylsilole. *Chem. Commun.*, (18), 1740–1741.

60 Chen, J., Law, C.C.W., Lam, J.W.Y., Dong, Y., Lo, S.M.F., Williams, I.D., Zhu, D., and Tang, B.Z. (2003) Synthesis, light emission, nanoaggregation, and restricted intramolecular rotation of 1,1-substituted 2,3,4,5-tetraphenylsiloles. *Chem. Mater.*, **15** (7), 1535–1546.

61 Hong, Y.N., Lam, J.W.Y., and Tang, B.Z. (2009) Aggregation-induced emission: phenomenon, mechanism and applications. *Chem. Commun.*, (29), 4332–4353.

62 Yan, M., Rothberg, L.J., Papadimitrakopoulos, F., Galvin, M.E., and Miller, T.M. (1994) Spatially indirect excitons as primary photoexcitations in conjugated polymers. *Phys. Rev. Lett.*, **72** (7), 1104–1107.

63 Yan, M., Rothberg, L.J., Kwock, E.W., and Miller, T.M. (1995) Interchain excitations in conjugated polymers. *Phys. Rev. Lett.*, **75** (10), 1992–1995.

64 Rothberg, L.J., Yan, M., Papadimitrakopoulos, F., Galvin, M.E., Kwock, E.W., and Miller, T.M. (1996) Photophysics of phenylenevinylene polymers. *Synth. Met.*, **80** (1), 41–58.

65 Greenham, N.C., Samuel, I.D.W., Hayes, G.R., Phillips, R.T., Kessener, Y.A.R.R., Moratti, S.C., Holmes, A.B., and Friend, R.H. (1995) Measurement of absolute photoluminescence quantum efficiencies in conjugated polymers. *Chem. Phys. Lett.*, **241** (1–2), 89–96.

66 Halls, J.J.M., Pichler, K., Friend, R.H., Moratti, S.C., and Holmes, A.B. (1996) Exciton diffusion and dissociation in a poly(*p*-phenylenevinylene)/C_{60} heterojunction photovoltaic cell. *Appl. Phys. Lett.*, **68** (22), 3120–3122.

67 Sheng, C.X., Tong, M., Singh, S., and Vardeny, Z.V. (2007) Experimental determination of the charge/neutral branching ratio η in the photoexcitation of π-conjugated polymers by broadband ultrafast spectroscopy. *Phys. Rev. B*, **75** (8), 085206.

68 Jenekhe, S.A. and Osaheni, J.A. (1994) Excimers and exciplexes of conjugated polymers. *Science*, **265** (5173), 765–768.

69 Jenekhe, S.A. (1995) Excited-state complexes of conjugated polymers. *Adv. Mater.*, **7** (3), 309–311.

70 Lemmer, U., Heun, S., Mahrt, R.F., Scherf, U., Hopmeier, M., Siegner, U., Göbel, E.O., Müllen, K., and Bässler, H. (1995) Aggregate fluorescence in conjugated polymers. *Chem. Phys. Lett.*, **240** (4), 373–378.

71 Blatchford, J.W., Gustafson, T.L., Epstein, A.J., Vanden Bout, D.A., Kerimo, J., Higgins, D.A., Barbara, P.F., Fu, D.K., Swager, T.M., and MacDiarmid, A.G. (1996) Spatially and temporally resolved emission from aggregates in conjugated polymers. *Phys. Rev. B*, **54** (6), R3683–R3686.

72 Conwell, E. (1997) Excimer formation and luminescence in conducting polymers. *Trends Polym. Sci.*, **5** (7), 218–222.

73 Grell, M., Bradley, D.D.C., Long, X., Chamberlain, T., Inbasekaran, M., Woo, E.P., and Soliman, M. (1998) Chain geometry, solution aggregation and enhanced dichroism in the liquid-crystalline conjugated polymer poly(9,9-dioctylfluorene). *Acta Polym.*, **49** (8), 439–444.

74 Nguyen, T.-Q., Martini, I.B., Liu, J., and Schwartz, B.J. (2000) Controlling interchain interactions in conjugated polymers: the effects of chain morphology on exciton-exciton annihilation and aggregation in MEH-PPV films. *J. Phys. Chem. B*, **104** (2), 237–255.

75 Nguyen, T.-Q., Kwong, R.C., Thompson, M.E., and Schwartz, B.J. (2000) Improving the performance of conjugated polymer-based devices by control of interchain interactions and polymer film morphology. *Appl. Phys. Lett.*, **76** (17), 2454–2456.

76 Sariciftci, N.S., Smilowitz, L., Heeger, A.J., and Wudl, F. (1992) Photoinduced electron-transfer from a conducting polymer to buckminsterfullerene. *Science*, **258** (5087), 1474–1476.

77 Yu, G., Gao, J., Hummelen, J.C., Wudl, F., and Heeger, A.J. (1995) Polymer photovoltaic cells: enhanced efficiencies via a network of internal donor-acceptor heterojunctions. *Science*, **270** (5243), 1789–1791.

78 Sariciftci, N.S., Heeger, A.J., and Nalwa, H.S. (eds) (1997) *Handbook of Organic*

Conductive Molecules and Polymers, vol. 1, John Wiley & Sons, Inc., New York.

79 Brabec, C.J., Zerza, G., Cerullo, G., De Silvestri, S., Luzzati, S., Hummelen, J.C., and Sariciftci, S. (2001) Tracing photoinduced electron transfer process in conjugated polymer/fullerene bulk heterojunctions in real time. *Chem. Phys. Lett.*, **340** (3–4), 232–236.